*J. exp. Biol.* 152, 211–241 (1990)
*Printed in Great Britain* © *The Company of Biologists Limited 1990*



# PLATEAU-GENERATING NERVE CELLS IN *HELIX*: PROPERTIES OF THE REPOLARIZING VOLTAGE-GATED AND $Ca^{2+}$-ACTIVATED POTASSIUM CURRENTS

BY M. CREST, E. EHILE, T. PIN, K. WATANABE AND M. GOLA*

*Laboratoire de Neurobiologie, CNRS, 31, Chemin Joseph-Aiguier, 13402 Marseille Cedex, France*

*Accepted 24 May 1990*

## Summary

The aim of this study was to identify and characterize the repolarizing currents present in *Helix* nerve cells that generate long-lasting $Ca^{2+}$-dependent depolarized plateaus in response to low-frequency stimulation. Two $K^+$ currents were identified: a voltage-gated K(V) current and a $Ca^{2+}$-activated $K^+$ current or C current. These currents were studied separately in cells injected with either EGTA, tetraethylammonium ($TEA^+$) or $Cs^+$. C current activation was found to be rate-limited by the size of the inward $Ca^{2+}$ current. Both K(V) and C currents displayed a pronounced relaxation during sustained depolarizations. Inactivation of the K(V) current was voltage-dependent. Inactivation of the C current was induced by either tiny $Ca^{2+}$ entries or intracellular $Ca^{2+}$ injections; C current inactivation was found to be more sensitive to intracellular $[Ca^{2+}]$ than the activating process. Similar experiments performed on various nerve cells revealed that the amount and rate of inactivation of both currents, but not their gating properties, varied greatly from cell to cell; plateau-generating cells had the strongest inactivating processes acting on both $K^+$ currents. These properties help to explain how regular firing may turn into long-lasting depolarized plateaus. They point to the existence of cellular processes that might regulate the number of available $K^+$ channels in a manner that is specific to the nerve cell type.

## Introduction

In a previous paper (Pin *et al.* 1990), we described the morphological and electrophysiological characteristics of a nerve cell group within the circumoesophageal ganglion of *Helix*. Upon sustained or repeated stimulation, these cells produced overshooting spikes that suddenly turned into prolonged depolarized plateaus lasting for several seconds. Because of their plateau-generating properties, these cells were styled P cells. Both spike and plateau were $Ca^{2+}$-dependent, since they persisted in $Na^+$-free saline and they were abolished by $Ca^{2+}$ channel

* To whom reprint requests should be addressed.

Key words: *Helix pomatia*, neurones, $Ca^{2+}$ current, $Ca^{2+}$-activated $K^+$ current, $Ca^{2+}$-induced inactivation.

blockers or in $Ca^{2+}$-free saline. A slowly inactivating $Ca^{2+}$ current has been detected in P cells. This $Ca^{2+}$ current undoubtedly sustained the long-lasting plateau.

Similar persistent $Ca^{2+}$ currents were observed in various nerve cells within *Helix* ganglia. Some of these cells were able to fire purely $Ca^{2+}$-dependent spikes (Lux and Hofmeier, 1982*a*) but failed to produce depolarized plateaus. These findings prompted the idea that P cells had specific outward currents that could not counteract the depolarizing tendency of the persistent $Ca^{2+}$ current.

In this paper, we have analysed the properties of the repolarizing outward currents present in the plateau-generating cells. Two components have been detected: a voltage-gated $K^+$ current and a $Ca^{2+}$-activated $K^+$ current. Both currents were characterized by pronounced inactivating processes triggered either by cell depolarization or by intracellular $Ca^{2+}$ accumulation. The existence of these processes helps us to understand how regular spiking may turn into uncontrolled depolarizations.

## Materials and methods

Some of the methods used here have been described in the preceding paper. Conventional voltage-clamp methods were used. Ionophoretic intracellular injections were performed while the cell was voltage-clamped so that no net current flowed through the membrane during injection. The microelectrodes used for intracellular injections were pulled from 1.5 mm glass capillary electrodes. They were filled with either 1 mol $l^{-1}$ TEACl, 3 mol $l^{-1}$ CsCl and 0.7 mol $l^{-1}$ EGTA ($K^+$ salt) or 10–50 mmol $l^{-1}$ $CaCl_2$. Calcium was also pressure injected from electrodes filled with 0.1 mol $l^{-1}$ $CaCl_2$ and 0.1 mol $l^{-1}$ KCl. Injection by pressure ($1\times10^5$–$3\times10^5$ Pa) was facilitated by applying a retention current (5–10 nA negative current; Hofmeier and Lux, 1981). Pipettes for pressure injection were pulled in three steps with a vertical puller (David Kopf, model 720) in a similar way to that used with patch-clamping electrodes. They had a tip diameter of 1 $\mu$m. Four microelectrodes could be introduced simultaneously into the same cell.

Experiments were performed in four plateau-generating cells located in the visceral and right parietal ganglia. A comparative study was conducted in three other nerve cell groups styled A cells, bursting cells (Br) and U cells (see Pin *et al.* 1990, for location and properties of these cells).

In all salines, the osmolarity was maintained at 200–210 mosmol $l^{-1}$ by adding appropriate amounts of Tris (pH 7.6). The composition of the standard saline was (in mmol $l^{-1}$): NaCl, 75; KCl, 5; $CaCl_2$, 8; $MgCl_2$, 8; Tris (pH 7.6), 5. In standard $Na^+$-free saline NaCl was replaced by 90 mmol $l^{-1}$ Tris. In $Na^+$-free $TEA^+$ saline, $Na^+$ was replaced by 60 mmol $l^{-1}$ $TEA^+$. When necessary 4-aminopyridine (4-AP) (5–10 mmol $l^{-1}$) was added to the various salines. The $Ca^{2+}$ channel blockers cadmium or lanthanum (0.5–2 mmol $l^{-1}$) were added to the $Ca^{2+}$-containing salines; cobalt (8 mmol $l^{-1}$) was substituted for $Ca^{2+}$. The preparation was continuously perfused at a constant rate (3 ml $min^{-1}$).

The data were sampled at 5–10 kHz, through a 16-bit A/D converter and they were stored on floppy disks. Any capacitative or leak currents occurring in response to step depolarizations were routinely eliminated by adding the current induced by 50 mV hyperpolarizing pulses, scaled at the appropriate level. If not otherwise stated, the holding potential was set at −50 mV. Experiments were performed at room temperature (20–22 °C).

## Results

### *Identification of the main ionic components*

The inward current in P cells flowed mainly through $Ca^{2+}$ channels. Replacement of $Na^+$ by an isosmotic amount of Tris did not significantly (less than 20 %) reduce the peak inward current triggered by short depolarizing pulses at 0 mV.

The outward current typically displayed a two-step activation time course: an initial fast component followed by a slowly activating component. The two phases were particularly prominent at large depolarizations. The superimposed recordings in Fig. 1A were from a P cell bathed in the standard $Na^+$-free saline. Currents were induced by 80 ms pulse depolarizations to −10 to +70 mV in 20 mV steps. To prevent cumulative inactivation of the outward current (see below), pulses were applied at a slow rate (every 20 s). The cell was then impaled with an EGTA-filled microelectrode. Immediately after impalement, the slow current component was reduced. Passive diffusion of EGTA generally sufficed to block the slow component fully. Blockade was speeded up by ionophoretic injection with negative current pulses (50 nA, 500 ms, 1 Hz) for 2–4 min. The progressive effect of EGTA on the outward current is shown in the inset in Fig. 1B.

The outward current which persisted after EGTA had the same properties as the voltage-dependent delayed rectifier, with a fast activation rate at large positive potentials (Fig. 1B). The current suppressed by EGTA had the main characteristics of the $Ca^{2+}$-dependent $K^+$ current described in *Helix* neurones (Woolum and Gorman, 1981; Lux and Hofmeier, 1982*a*). Unlike the voltage-dependent $K^+$ component, its activation rate decreased at large positive potentials (Fig. 1C).

The outward current resistant to intracellular EGTA was then blocked by adding 60 mmol $l^{-1}$ $TEA^+$ to the $Ca^{2+}$-free saline. The progressive effect of $TEA^+$ on the current at 0 mV is shown in Fig. 1D,E. The blockade of the outward current unmasked a slowly inactivating inward current which was fully suppressed by bathing the cell in the $Na^+$-free $TEA^+$ saline in which $Co^{2+}$ was substituted for $Ca^{2+}$ (Fig. 1F).

It therefore emerged that the net ionic membrane current in the P cells had five components: the inward current flowed mainly through $Ca^{2+}$ channels; the $Na^+$ current amounted to 10–20 % of the inward current, and therefore did not greatly determine the electrical behaviour of the P cells (see Pin *et al.* 1990). The outward current also had two components, each contributing about 50 % to the total outward current: an EGTA-sensitive current that we will call the C current and an EGTA-insensitive, $TEA^+$-sensitive current, which had the properties of the

voltage-dependent delayed rectifier. The voltage-dependent $K^+$ current will be styled the K(V) current. The fast transient A current was also present in P cells. Its activation produced the break response (Gola and Romey, 1971) observed upon fast depolarization in P cells that had a more negative resting potential than −50 mV. The A current was routinely suppressed under voltage-clamp conditions

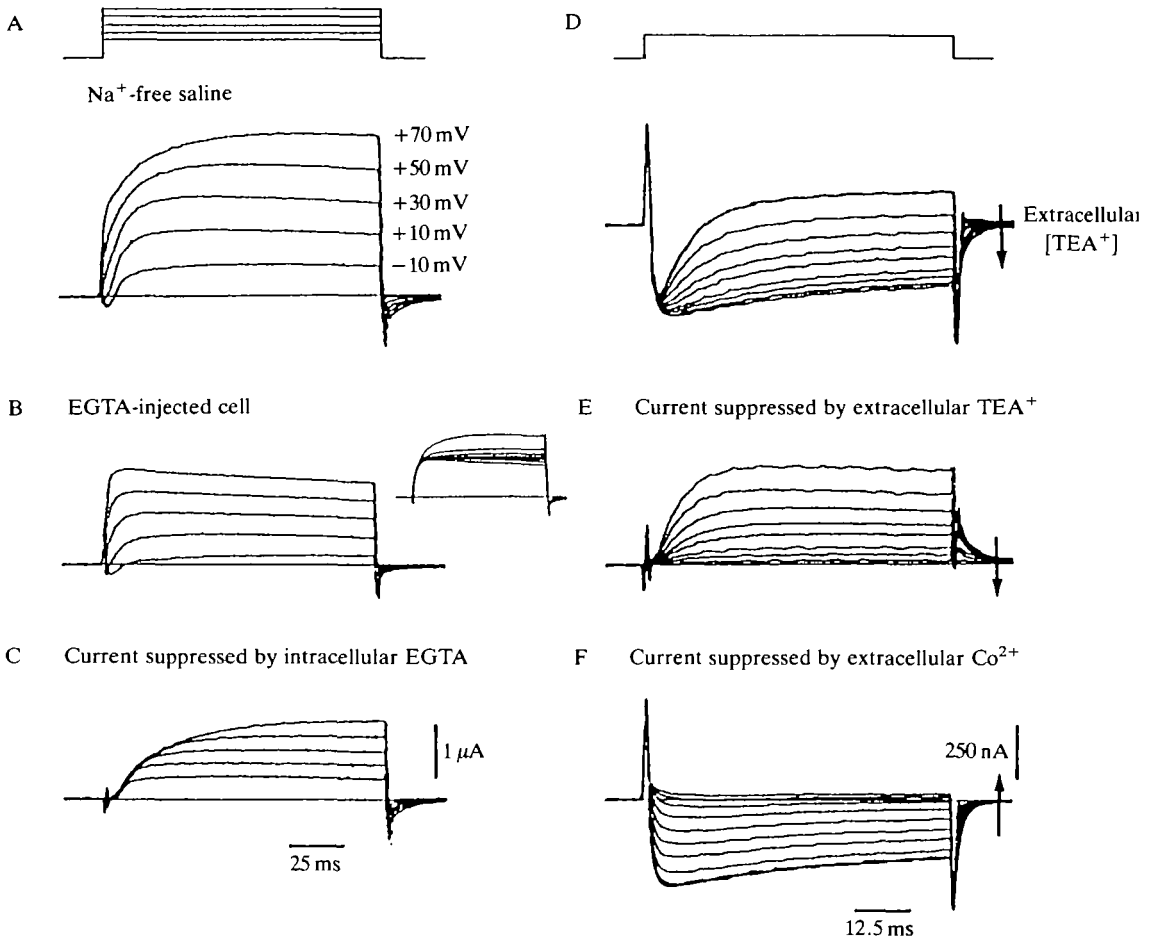


Fig. 1. Potassium and calcium currents in P cells. (A,B) Superimposed currents in response to pulse depolarizations (at the levels indicated) performed before (A) and after (B) intracellular injection of EGTA. Cell bathed in $Na^+$-free saline. Holding potential: −50 mV. The EGTA-filled microelectrode was inserted just after recordings A. The progressive effect of EGTA injection on the +50 mV current is shown in inset B. (C) Current suppressed by EGTA (series A minus series B). The cell was then bathed in 60 mmol $l^{-1}$ $TEA^+$ saline, which progressively suppressed an outward current. (D) Progressive effect of extracellular $TEA^+$ on the current induced by a test pulse at 0 mV. (E) Same series minus the TEA-resistant current. (F) The inward current revealed by intracellular EGTA and extracellular $TEA^+$ was progressively blocked by substituting $Co^{2+}$ (8 mmol $l^{-1}$) for $Ca^{2+}$ in the $TEA^+$ saline. In D–F current changes are outlined by vertical arrows.

by setting the holding potential to −50 mV. The A current, however, was found to be sensitive to the divalent ion content of the saline; its activation and inactivation thresholds could be shifted to positive potentials by raising the $Ca^{2+}$ and/or $Mg^{2+}$ contents of the saline (Tsuda *et al.* 1988). To prevent activation of the A current, 5–10 mmol $l^{-1}$ 4-AP, which selectively blocked the A current, was added to the various salines.

The C current component was also identified by its sensitivity to $Ca^{2+}$-channel blockers, i.e. $Cd^{2+}$ (0.5 mmol $l^{-1}$) or $La^{3+}$ (1 mmol $l^{-1}$) added to the $Na^+$-free saline, or $Co^{2+}$ substituted in equimolar amounts for $Ca^{2+}$. $Ca^{2+}$ channel blockers specifically suppressed the slow component of the outward current (Fig. 2A).

The current–voltage relationship of the C current was determined by subtract-

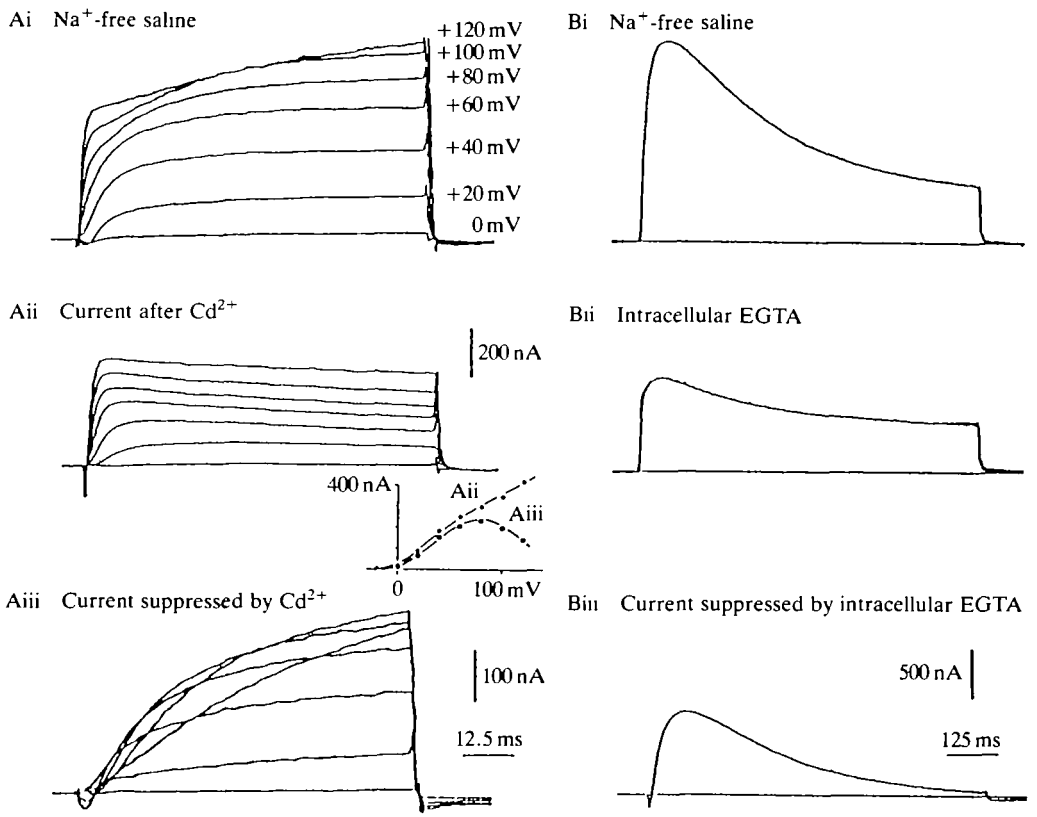


Fig. 2. The calcium-dependent $K^+$ current. (A) $Ca^{2+}$ channel blockers suppressed the slow outward current component. (Ai) Superimposed currents in response to 80 ms depolarizations at the levels indicated. Holding potential −50 mV. (Aii) Same series after adding 0.5 mmol $l^{-1}$ $Cd^{2+}$ to the $Na^+$-free saline. (Aiii) $Cd^{2+}$-sensitive current obtained by subtracting series Aii from series Ai. Inset: current–voltage curves corresponding to series Aii and Aiii. (B) Effect of long-lasting (0.7 s) depolarizations on $K^+$ currents. Test pulse +30 mV. (Bi) Total outward current. (Bii) K(V) current resistant to intracellular EGTA. (Biii) C current suppressed by EGTA (Bii minus Bi).

ing the currents remaining after $Ca^{2+}$ channel blockade from the corresponding currents recorded in control saline (Fig. 2Aiii). In control $Na^+$-free saline, the current–voltage relationship of the outward current was N-shaped. The N shape disappeared in the presence of $Ca^{2+}$ channel blockers. The C current amplitude increased over the range −30 to +50 mV. It decreased at larger depolarizations with an extrapolated null-current potential located at +120–140 mV (inset in Fig. 2A). Because of the kinetic changes that affected the C current at large positive potentials, the voltage that produced a maximal C current was actually dependent on the test pulse duration (see Lux and Hofmeier, 1982*a*). This voltage was positively shifted when the test pulse lengthened. These properties are typical of the $Ca^{2+}$-activated $K^+$ current originally described by Meech and Standen (1975) in *Helix* neurones and further identified in various molluscan nerve cells (Woolum and Gorman, 1981; Lux and Hofmeier, 1982*a*,*b*).

The activation time course of the C current differed markedly from that of the voltage-dependent component, which had fast kinetics at positive potentials. At moderate depolarization, the C current had a relatively fast onset with a peak occurring in 30–50 ms. The activation rate decreased at large depolarizations. The current became very slow at potentials corresponding to the decreasing part of the C current–voltage curve (Fig. 2Aiii).

In long-lasting (0.5–0.8 s) depolarizations, the outward current displayed a relatively fast relaxation which reduced its level by 60–70 %. The relaxation was observed whatever the membrane potential. Both voltage-gated $K^+$ current and the C current were involved. Fig. 2Bi shows the net outward current at +30 mV from a P cell bathed in the $Na^+$-free saline. The depolarizing pulse lasted 0.7 s. The C current was then blocked by intracellular injection of EGTA. The EGTA-resistant current had a relaxation that affected 50–70 % of the peak current (Fig. 2Bii). The current suppressed by intracellular EGTA was also reduced by the 0.7 s depolarizing pulse (Fig. 2Biii), particularly at potentials that produced large $Ca^{2+}$ entries (from 0 to +30 mV).

In most *Helix* nerve cells the compound outward current displayed a fairly prominent relaxation. We have observed that P cells belong to a group of nerve cells characterized by fast and large relaxation. This finding was used as an additional criterion for identifying P cells.

### *Pharmacological separation of the two $K^+$ currents*

To determine the properties of the C current, we looked for pharmacological agents that were able specifically to block the voltage-dependent component. Extracellularly applied 4-AP (10 mmol $l^{-1}$) and apamin (0.1 mmol $l^{-1}$) had little or no effect on either $K^+$ current, whereas extracellular $TEA^+$ blocked both components (Fig. 3A). The $Ca^{2+}$-dependent component, however, was much more sensitive to $TEA^+$ (apparent dissociation constant $K_d \approx 1$ mmol $l^{-1}$) than was the voltage-dependent component ($K_d \approx 20$ mmol $l^{-1}$), in agreement with the data of Hermann and Gorman (1981). Even in the presence of 60 mmol $l^{-1}$ $TEA^+$, the voltage-dependent current could not be fully suppressed.

The voltage-dependent $K^+$ current was found to be sensitive to intracellular $TEA^+$. $TEA^+$ was ionophoretically injected from a 1 mol $l^{-1}$ $TEA^+$-filled microelectrode. Immediately after cell penetration with the $TEA^+$ electrode, the fast current component started to decrease. Further reduction was obtained with a 5–10 min ionophoretic injection (50–100 nA, positive current). During the injection period, the slow C current remained unchanged (Fig. 3B). More prolonged $TEA^+$ injections, however, had a moderate blocking effect on the C current (see also Hermann and Gorman, 1981).

The effects of intracellular $TEA^+$ on the voltage-dependent $K^+$ current were assessed as follows. A P cell bathed in the $Na^+$-free saline was first injected with $TEA^+$ for 5–10 min. The C current component was then suppressed by an intracellular injection of EGTA from a fourth electrode filled with EGTA. Under these conditions, a small outward current still persisted. This outward current was then suppressed by bathing the cell in the $TEA^+$ (60 mmol $l^{-1}$) $Na^+$-free saline. Currents successively collected under these conditions are shown in Fig. 3D, in which test pulses were at +20 and +60 mV. Full blockade of the $K^+$ currents by

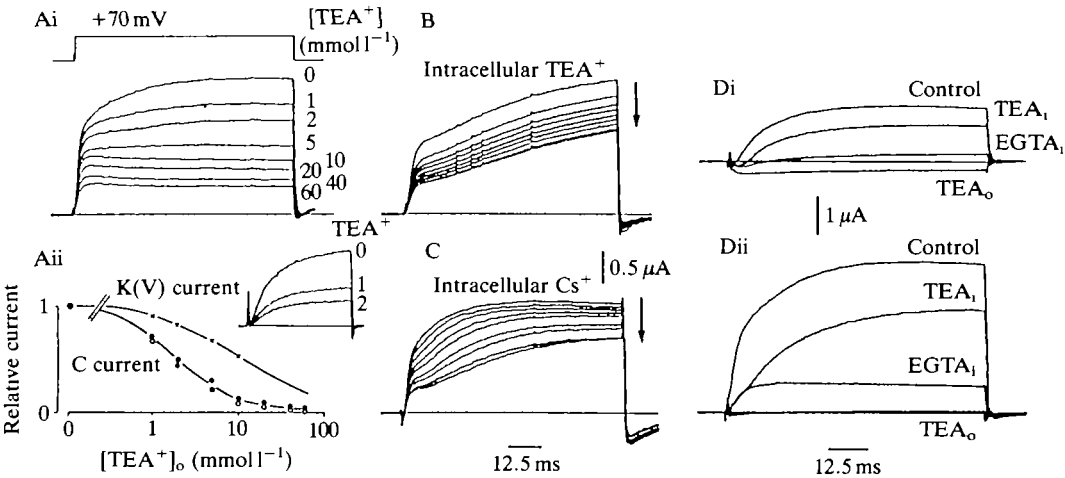


Fig. 3. Pharmacological separation of $Ca^{2+}$-activated and voltage-gated $K^+$ currents in P cells. (A) Effect of extracellular $TEA^+$. (Ai) Total outward current induced by pulse depolarizations at +70 mV. The slow component was almost fully blocked by 5 mmol $l^{-1}$ extracellular $TEA^+$. Inset shows the effect of low $TEA^+$ concentrations on the C current. Data are summarized in Aii: $K_d$ (apparent dissociation constant) for C and K(V) currents are 1–2 and 10 mmol $l^{-1}$ $TEA^+$, respectively. (B,C) Blockade of the K(V) current by intracellularly injected $TEA^+$ (B) or $Cs^+$ (C). In both figures the top trace was recorded before inserting the TEACl- or CsCl-filled electrode. Injection was then performed ionophoretically (change in current outlined by arrows). Test pulses B, +60 mV; C, +80 mV. Ionophoretic injection with 30–50 nA positive current pulses for 8 min (B) and 15 min (C). (D) Currents in both series were successively recorded in the $Na^+$-free saline (control), after intracellular injection of $TEA^+$ ($TEA_i$), after intracellular injection of EGTA ($EGTA_i$) or after bathing the cell in 60 mmol $l^{-1}$ $TEA^+$ saline ($TEA_o$). Pulse levels: +20 mV in Di and +60 mV in Dii.

the combined effects of intracellular $TEA^+$, intracellular EGTA and extracellular $TEA^+$ unmasked the persistent $Ca^{2+}$ current (Fig. 3Di). The current suppressed by extracellular $TEA^+$ had the properties of the outward current suppressed by intracellular $TEA^+$; i.e. both currents contributed to the voltage-dependent $K^+$ current. Therefore, in spite of its great sensitivity to intracellular $TEA^+$, the voltage-dependent $K^+$ current could not be fully suppressed by long-lasting $TEA^+$ injections (see Heyer and Lux, 1976).

We also tried to block selectively the voltage-dependent component with intracellular $Cs^+$. Immediately after cell penetration with a 3 mol $l^{-1}$ CsCl-filled electrode, the voltage-dependent $K^+$ component decreased. It was then almost fully blocked by a 10–20 min ionophoretic injection (Fig. 3C). As with intracellular $TEA^+$, the $Ca^{2+}$-dependent component remained unaltered. Larger injections, however, tended to block the C current. There was an overlap between the injection required to block the voltage-dependent component and those that had already affected the C current. This overlap was less prominent with $TEA^+$; the intracellular $TEA^+$-sensitive component could be fully suppressed without noticeably affecting the C current. We therefore routinely used $TEA^+$-injected P cells to study the properties of the C current, although we knew that a small proportion of the outward current was still contributed by unblocked voltage-dependent $K^+$ channels. Routine injections of $TEA^+$, performed with 40–50 nA for 10–12 min, reduced voltage-gated $K^+$ currents by 75–85 % in a voltage-independent manner.

*Properties of the voltage-activated $K^+$ current*

Experiments were performed on P cells bathed in the $Na^+$-free, $Ca^{2+}$-free saline containing 8 mmol $l^{-1}$ $Co^{2+}$ and 10 mmol $l^{-1}$ 4-AP, in order to suppress $Na^+$, $Ca^{2+}$, C and A currents.

The activation rate of the voltage-dependent $K^+$ current was studied using short (50–80 ms) depolarizing pulses. The activation threshold was about −20 mV. The peak current increased with the depolarizing pulse amplitude while its onset became faster (Fig. 4Ai). On depolarization the increase in the current had an S-shaped time course. Analysis of these onset records has shown that the time course of activation was well-fitted by an exponential function raised to the second power (Connor and Stevens, 1971):

$$I_{K(V)} = \bar{I}_{K(V)}[1 - \exp(-t/\tau)]^2,$$

where $\bar{I}_{K(V)}$ is the peak value of the K(V) current and $\tau$ is the time constant of activation. The continuous curves through the experimental points in Fig. 4Ai were drawn on the basis of this relationship. The time constant $\tau$ was found to be highly voltage-dependent, decreasing from 50 ms at 0 mV to 2 ms at +100 mV. Data from four different P cells are summarized in Fig. 4Aii.

The same analysis was performed on other identified neurones. No difference in the activation parameters could be detected, i.e. the voltage-dependent $K^+$ current in P cells seemed to be identical to that already described in molluscan neurones (Reuter and Stevens, 1980).

During sustained depolarization the K(V) current decreased. After 800 ms of depolarization, 60–80 % of the current was blocked. The decrease was not paralleled by any significant shift in the current reversal potential and it persisted when $[K^+]_o$ was increased to 80 mmol $l^{-1}$, which excluded the possibility of $K^+$ accumulation being the primary cause of current relaxation. Slow inactivating processes acting on voltage-gated $K^+$ currents in molluscs have been well documented (see Aldrich, 1981; Ruben and Thompson, 1984).

The steady-state inactivation curve was determined by applying a 5–10 s conditioning potential at various levels just before a test depolarizing pulse. Results from one such experiment are displayed in Fig. 4B. The peak K(V) current decreased with holding potentials ranging from −60 to 0 mV. Part of the

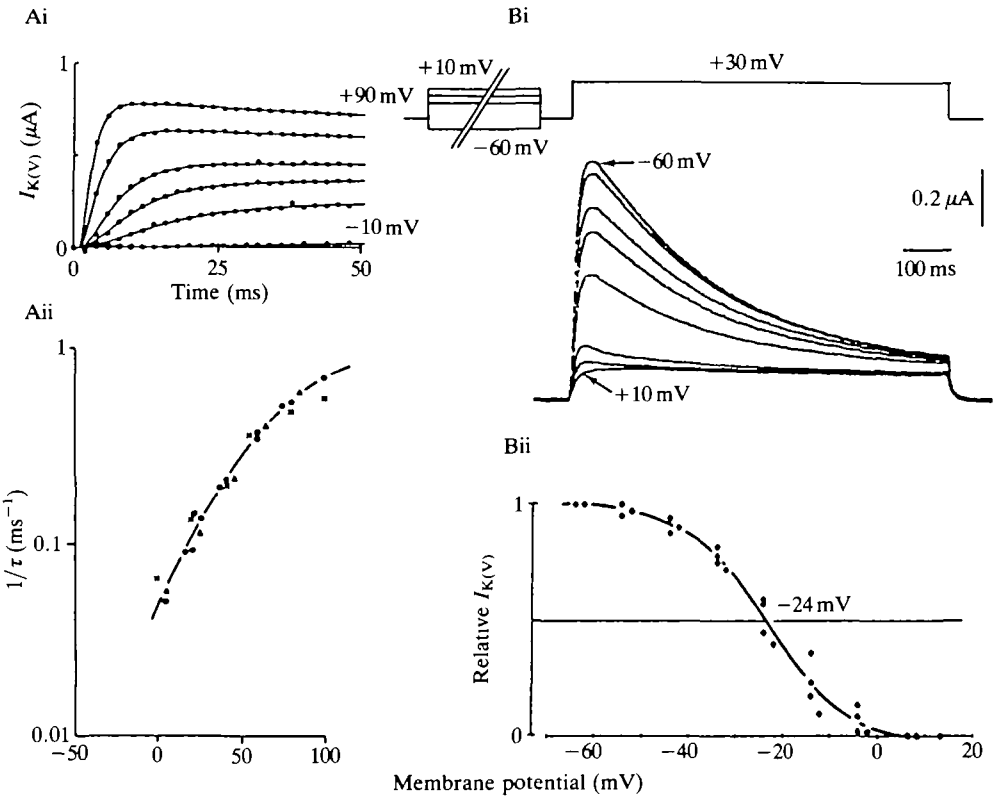


Fig. 4. Properties of the voltage-gated K(V) current in P cells. (A) Activation parameters. (Ai) K(V) current at various potentials (in 20 mV steps) in a P cell bathed in $Na^+$- and $Ca^{2+}$-free $Co^{2+}$ (8 mmol $l^{-1}$) saline. Continuous curves through experimental points are squared exponential functions. (Aii) Plot of the reciprocal of the activation time constant *versus* membrane potential (data pooled from four P cells). (B) Voltage-dependent inactivation. (Bi) K(V) currents in response to a 0.8 s depolarization at +30 mV applied 0.5 s after a 10 s conditioning pulse at potentials ranging from −60 to +10 mV. (Bii) Plot of the inactivating peak K(V) current *versus* the conditioning potential; results pooled from four P cells. Continuous curve drawn according to a Boltzmann distribution (see text).

current, however, could not be blocked by large conditioning depolarizations. This non-inactivating current corresponded to the steady-state current level reached after prolonged depolarization. The inactivating current in P cells corresponded to 80–90 % of the total voltage-dependent $K^+$ current.

The steady-state inactivation curve was obtained by plotting the peak of the inactivating current (non-inactivating current subtracted) as a function of the conditioning potential. Results from four P cells are shown in Fig. 4Bii. The continuous curve fitted through the data points is a Boltzmann distribution which is given by:

$$\text{Relative } I_{K(V)} = \{1 + \exp[(V - V_0)/k]\}^{-1},$$

where $k$ is the slope factor.

The steady-state inactivation curve had a half-inactivation voltage $V_0$ at −24 mV and a slope factor $k$ of 8 mV. The same values were obtained in different nerve cell types in the visceral and parietal ganglia. They are similar to those reported in various molluscan neurones (Kostyuk *et al.* 1975; Aldrich *et al.* 1979).

On the basis of the steady-state inactivation and activation parameters, the voltage-dependent $K^+$ current in P cells was found to be identical to the corresponding current in other nerve cells. The kinetics of inactivation, however, were found to be very variable. During 800 ms depolarizing pulses, the K(V) current in P cells relaxed to 60–80 % of its peak value. The inactivation was almost exponential, with time constants of 250–400 ms. A comparative study was performed on 80 different neurones. The inactivation, evaluated from the level of relative current decrease in 800 ms depolarizations, ranged between 20 and 75 %. Cells with reduced inactivation (20–40 % inactivation in 800 ms) were characterized by slow inactivation kinetics (time constants of 1–1.6 s). There was no correlation between the speed of inactivation and the amount of inactivation recorded in long (5–10 s) depolarizations.

Judging from the location of the inactivation curve and the amount of inactivation in long-lasting depolarizations, the inactivating process of the voltage-dependent $K^+$ current in various nerve cells seemed to have similar steady-state properties. The speed with which the inactivation developed, however, varied greatly and therefore did not seem to be directly determined by the membrane potential. This variability has been observed by several investigators (Heyer and Lux, 1976; Aldrich *et al.* 1979). The fastest inactivating process was found to occur in P cells and in the large A cells located in the rostral part of the parietal ganglia (see Pin *et al.* 1990). In these cells, the recovery from inactivation had a two-exponential time course. Both components were strongly voltage-dependent; the recovery became faster when the cell was held at potentials more negative than −60 mV. Near −50 mV, the recovery was a slow process: the time constants of the two exponential phases were 0.4 and 3.5 s. The relative contribution of the slow component of recovery was 60–70 %. Therefore, full recovery from inactivation required 10–20 s rest periods between successive tests.

The fact that K(V) currents in P cells inactivated rather quickly and that

inactivation required long resting periods for full recovery made this current very sensitive to repeated pulsing. Even at frequencies of 0.5–1 Hz, repetitive pulsing produced cumulative inactivation, which strongly depressed the available K(V) current.

*Calcium limits the C current activation rate*

The slowing down of the C current onset at large depolarization might result either from a peculiar voltage dependence of channel opening (Lux and Hofmeier, 1982*b*) or from the reduced $Ca^{2+}$ inflow that occurred under these conditions. According to the rate-limiting hypothesis, it was expected that the C current would have slow kinetics in potential ranges producing small $Ca^{2+}$ currents. This was the case when the potential was set to large positive values. Data concerning moderate depolarizations (from −30 to 0 mV) that induced small $Ca^{2+}$ entries were collected as follows. In this potential range, inward and outward currents had similar magnitudes and C and K(V) currents both had a slow onset, which obscured the contribution of the C current. This contribution was measured by successively injecting $TEA^+$ (large injection of 15–20 min, 50 nA) and then EGTA. Pre-injection currents were determined just before inserting the corresponding electrode. The current suppressed by intracellular EGTA (10 min injection, −50 nA) is shown in Fig. 5A.

The intracellular-EGTA-sensitive current had a threshold of about −25 mV. At all voltages, this current had a sigmoidal onset which could not be satisfactorily fitted to exponential functions raised to the second or third power. These functions gave latencies that were significantly shorter than those observed. Better fits were obtained with two independent exponential functions (not shown). The C current amplitude increased with voltage, whereas its activation rate decreased at large positive potentials as already described. In the negative potential region, this current also had a slow activation rate. Data are summarized in the diagram in Fig. 5B, in which the activation rate was estimated from the time required for half-activation. This time had a minimum value of 6–8 ms at voltages that produced a large $Ca^{2+}$ entry. The peak $Ca^{2+}$ current in the same $TEA^+$-EGTA-injected cell is shown in Fig. 5C. The U-shaped time-constant–voltage curve of the C current differed remarkably from the bell-shaped curve observed for most voltage-gated $K^+$ currents. Near 0 mV, the C current had a half-activation time of 6–8 ms. The corresponding value for the voltage-activated $K^+$ current was 20–25 ms. The C current was therefore 3–4 times faster than the K(V) current. The opposite situation prevailed at positive potentials. The time to half-activation at +60 mV was 12–20 ms for the C current and 3 ms for the voltage-activated $K^+$ current.

The hypothesis that a rate-limiting role may be played by calcium was also checked by altering the magnitude of the $Ca^{2+}$ current at a given membrane potential. This was done by changing the $Ca^{2+}$ concentration in $Na^+$-free saline. Divalent ions, however, have non-specific modulatory effects on most channels by screening negative membrane charges. These non-specific effects were minimized

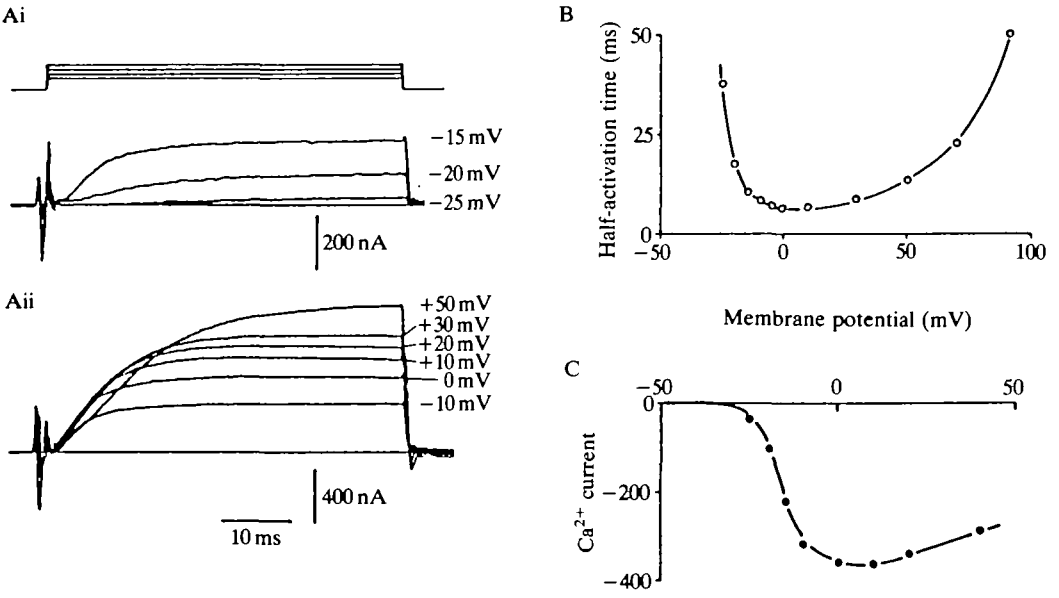


Fig. 5. C current activation kinetics. C current isolated by intracellular injection of EGTA in a $TEA^+$-injected cell bathed in the standard $Na^+$-free saline. Currents suppressed by intracellular EGTA are shown in series A with 80 ms pulse depolarizations ranging from −25 to +50 mV. The C current had a slow onset at either reduced or large depolarizations. Data are summarized in B; ordinate: time to half-activation; abscissa: pulse potential. (C) The peak $Ca^{2+}$ current induced by the test pulse was then obtained by bathing the EGTA–$TEA^+$-injected cell in 60 mmol $l^{-1}$ $TEA^+$ saline. Fast C current onset occurred at potentials producing large $Ca^{2+}$ currents.

by keeping the total divalent ionic content constant. $Ca^{2+}$ (from 0 to 16 mmol $l^{-1}$) was substituted in equimolar amounts for $Mg^{2+}$.

The results shown in Fig. 6A were from a $TEA^+$-injected P cell. Superimposed recordings in Fig. 6Ai show the parallel effect of reduced $Ca^{2+}$ concentrations on both $Ca^{2+}$ current and outward current triggered by +10 mV depolarizing pulses. The effect on the activation time course of the C current was better demonstrated by setting the depolarizing pulse at large positive levels. Fig. 6Aii, Aiii shows the time course of the C current at +50 mV, in the presence of various $[Ca^{2+}]_o$ (Fig. 6Aii) and during the change from 8 mmol $l^{-1}$ $[Ca^{2+}]_o$, 8 mmol $l^{-1}$ $[Mg^{2+}]_o$ to 0 mmol $l^{-1}$ $[Ca^{2+}]_o$, 16 mmol $l^{-1}$ $[Mg^{2+}]_o$ (Fig. 6Aiii). Low $[Ca^{2+}]_o$ reduced the peak C current and slowed down its activation rate. Similar results were obtained when $[Mg^{2+}]_o$ was kept constant at 8 mmol $l^{-1}$ and $[Ca^{2+}]_o$ was changed from 0 to 16 mmol $l^{-1}$. This ruled out the possibility that $Mg^{2+}$ may have affected the C current activation process. In the presence of 0 mmol $l^{-1}$ $[Ca^{2+}]_o$ 16 mmol $l^{-1}$ $[Mg^{2+}]_o$, no C current could be observed.

These data showed that the $Ca^{2+}$ inflow regulated both the amplitude and the activation rate of the C current. Although the effect on the activation rate was observed over the whole range of $[Ca^{2+}]_o$ changes, the peak C current saturated

when $[Ca^{2+}]_o$ was above 4 mmol $l^{-1}$. It therefore seemed that the peak C current was limited by the membrane potential, in agreement with the data by Lux and Hofmeier (1982*b*), whereas its activation rate was limited by the $Ca^{2+}$ inflow.

This hypothesis was confirmed by the data in Fig. 6B, which were obtained from a $TEA^+$-injected P cell. A slow C current was induced by a depolarizing pulse to +60 mV. The $Ca^{2+}$ current had a maximum peak value at voltages in the range +10 to +30 mV. Therefore the +60 mV pulse produced a limited $Ca^{2+}$ entry,

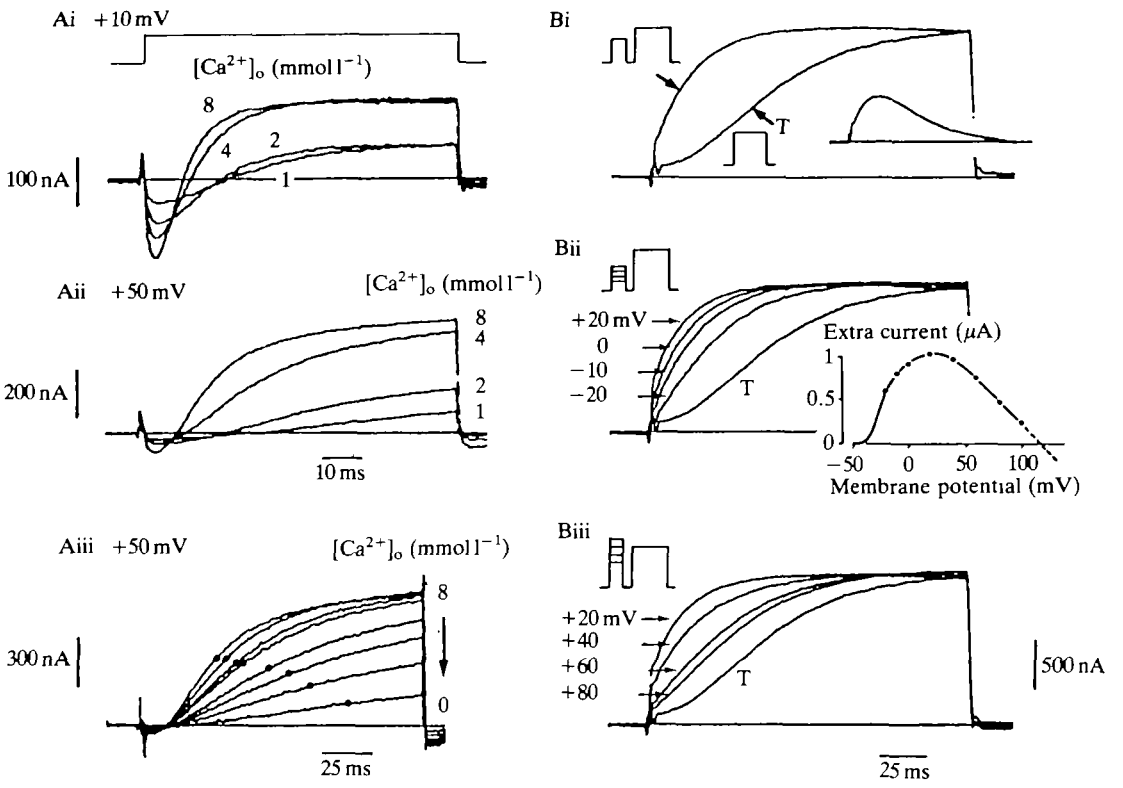


Fig. 6. $Ca^{2+}$ regulates the C current activation rate. (A) Effects of changes in the $Ca^{2+}$ content of the $Na^+$-free saline. $Ca^{2+}$ substituted for $Mg^{2+}$ to keep the divalent ionic content constant. $TEA^+$-injected P cell. $TEA^+$-resistant K(V) current eliminated by subtracting the current which persisted in 0 mmol $l^{-1}$ $[Ca^{2+}]_o$. (Ai, Aii) Change in $Ca^{2+}$ and C currents with changing $[Ca^{2+}]_o$ at two potential levels. (Aiii) Progressive decrease and slowing down of the C current (test pulse +50 mV) when $[Ca^{2+}]_o$ was step changed from 8 to 0 mmol $l^{-1}$. Dots indicate half-activation. (B) Increase in C current activation rate induced by $Ca^{2+}$ loading. Superimposed currents during a +60 mV test pulse in a $TEA^+$-injected cell. The slow C current induced by the test pulse is labelled T. In Bi it turned into a fast current when the test pulse was applied 40 ms after a short (30 ms) conditioning pulse at 0 mV. (Bii, Biii) Change in the C current activation rate with the conditioning pulse. Increasing the conditioning pulse first speeded up (Bii) then slowed down (Biii) the C current. Conditioning pulse level indicated on current traces. Inset in Bi, extra current (facilitated minus test current). Inset in Bii, peak extra current *versus* conditioning potential.

which accounted for the slow C current time course. When the test pulse was preceded by a short (20–30 ms) conditioning pulse at +10 mV, it dramatically speeded up the C current during the test pulse (Fig. 6Bi). The peak current was not altered, i.e. slow and fast C currents had the same limit value. The facilitating effect on the C current onset was directly related to the size of the $Ca^{2+}$ current induced by the conditioning pulse. A progressive increase in the C current activation rate was observed when conditioning potentials were changed from −50 to +20 mV (Fig. 6Bii). The reverse change occurred with conditioning potentials larger than +20 mV (Fig. 6Biii). The facilitating effect was assessed from the magnitude of the extra current obtained by subtracting the test current from the facilitated currents. One such extra current is shown in the inset in Fig. 6Bi. The extra current–voltage relationship (inset in Fig. 6Bii) had a peak at +20 mV and an extrapolated null-current potential in the range +100 to +120 mV. These figures were to be expected if C current facilitation was related to the size of the $Ca^{2+}$ current induced by the conditioning pulse.

The experiments reported in this section were also performed on U cells in which the $Ca^{2+}$-activated $K^+$ current displayed no sign of voltage- or $Ca^{2+}$-induced inactivation (Lux and Hofmeier, 1982*a*). Unlike P cells, U cells (as well as bursting cells) had C currents that persisted during 5–10 s depolarizations. The absence of inactivation in these C channels has been confirmed by recording unitary currents (Chagneux *et al.* 1989). Nevertheless, the C current activation in U cells displayed the same dependence on calcium influx as that in P cells.

*C current inactivation*

It has already been mentioned that the C current displayed a fast relaxation during prolonged depolarization. The relaxation was almost exponential. Its speed had maximal values at potentials ranging from 0 to +40 mV. A parallelism was found to exist between the change in activation and inactivation rates; with large depolarizations producing slowly rising C currents, the relaxation became slow (Fig. 7A).

On the basis of the $Ca^{2+}$ sensitivity, voltage dependency and activation kinetics, similar C currents were identified in almost all the neurones tested. The C current in P cells was found, however, to have the fastest inactivating process. For instance, the C current present in the purely $Ca^{2+}$-dependent U cells (Lux and Hofmeier, 1982*a*) did not relax even after several seconds of depolarization. The same was true of the C current in bursting neurones. Many other neurones displayed intermediate characteristics, i.e. they had C currents with moderate relaxation rates.

The steady-state C current inactivation–voltage relationship was determined in two steps. In a P cell bathed in the standard $Na^+$-free saline, a test pulse (+40 to +60 mV, 80 ms) was delivered after a 5–10 s conditioning pulse at various potential levels. Increasing the conditioning pulse amplitude produced a progressive blockade of the compound C and K(V) currents (Fig. 7Bi). The sequence was then repeated after intracellular injection of EGTA (Fig. 7Bii). The plot of the peak

outward current in the EGTA-injected cell gave the steady-state inactivation curve of the voltage-dependent component. The EGTA-resistant current was then subtracted from the corresponding current obtained before EGTA injection (Fig. 7Biii). The curve for the EGTA-sensitive current or C current and that for the EGTA-insensitive or K(V) current are shown in Fig. 7C. The C current had a very sharp steady-state inactivation curve. Inactivation was induced by membrane potentials ranging from −45 to −30 mV. Under similar conditions, the steady-state inactivation curve of the voltage-dependent component was located between −50 and 0 mV. Half-inactivation was induced by conditioning membrane potentials at −38± 2 mV ($N$=14), in the case of the C current, and −24±2.5 mV ($N$=12) in the case of the K(V) current. Assuming a Boltzmann distribution in the inactivated state, the steady-state inactivation curve of the C current would have a

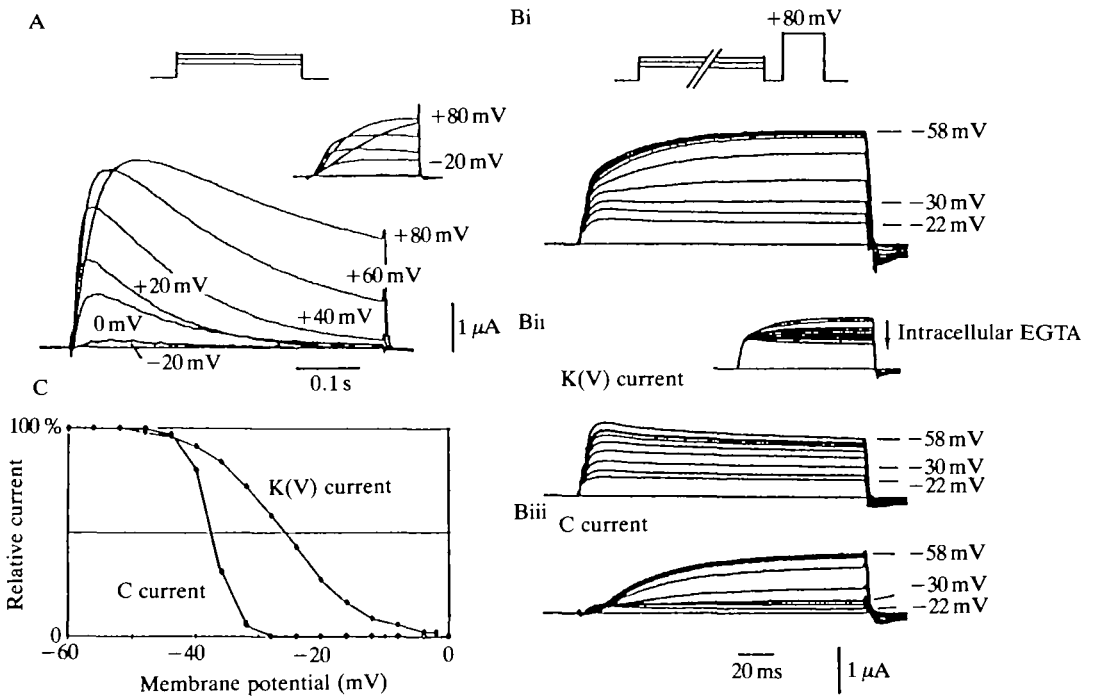


Fig. 7. C current inactivation in P cells. (A) Superimposed C currents induced by 0.8 s depolarizing pulses at the levels indicated. Corresponding onsets are shown in inset (80 ms pulses). $TEA^+$-injected cell. $TEA^+$-resistant K(V) current subtracted. (B) Effect of long conditioning depolarizations on C and K(V) currents. Currents in response to a test pulse (+80 mV) applied 0.1 s after a 10 s conditioning depolarization at various levels. In the three series the conditioning potential was changed from −58 to −22 mV, in 4 mV steps. (Bi) Cell in the standard $Na^+$-free saline. (Bii) K(V) current after EGTA injection; progressive effect of EGTA shown in inset. (Biii) C current obtained by subtracting series Bii from series Bi. (C) Relative peak C and K(V) currents (from series Bii and Biii, respectively) *versus* conditioning potential. Inactivation of the C current occurs in a narrow range of potentials, between −40 and −30 mV.

slope factor, $k$, of 2.5 mV. This shaping factor gave an estimate of the large voltage-sensitivity of the inactivating process that increases e-fold per 2.5 mV depolarization.

The C current blockade which followed a long-lasting conditioning depolarization might merely have resulted from inactivation of the $Ca^{2+}$ current. In most nerve cells, $Ca^{2+}$ currents are blocked by cell depolarization and/or intracellular $Ca^{2+}$ accumulation (Eckert *et al.* 1981). To check this possibility, the above conditioning paradigm was applied to a $TEA^+$-injected P cell bathed in 60 mmol $l^{-1}$ $TEA^+$ saline. $Ca^{2+}$ currents were induced by test pulses (about 0 mV) applied immediately after a 5–10 s conditioning depolarization. The test $Ca^{2+}$ current was progressively reduced by increasing conditioning depolarizations, along a Z-shaped curve. The voltage threshold inducing inactivation was around −40 mV and that for half-inactivation was $-24\pm2$ mV ($N=14$). No change in these values occurred after intracellular injection of EGTA. In the potential range which induced blockade of the C current, the $Ca^{2+}$ current was only slightly reduced. Conditioning depolarization at −30 mV fully suppressed the C current, whereas a large $Ca^{2+}$ current was still induced by the test pulse. We concluded that the blockade of the C current induced by long-lasting depolarizations in the −40 to −30 mV range did not result from blockade of the $Ca^{2+}$ current.

### *$Ca^{2+}$-induced delayed blockade of the C current*

As reported above, the C current was speeded up by a short depolarizing pulse producing a $Ca^{2+}$ entry. The $Ca^{2+}$-induced facilitating effect vanished when the interval between $Ca^{2+}$ entry and test pulse increased. After 0.5–0.8 s, not only was this facilitating effect over but the peak C current was considerably depressed (Fig. 8Ai). The depressed C current had the same time course as the slow C current (Fig. 8Aii). Recovery to the control level started 1 s after the $Ca^{2+}$ entry and full recovery required 8–20 s. We will therefore denote the effects on C current induced by short conditioning pulses as early facilitation and delayed depression. In nerve cells in which the C current did not relax during sustained depolarization, no delayed depression occurred, whereas early facilitation was observed. These findings confirm that at least two C currents characterized by different inactivating processes exist in *Helix* nerve cells.

The delayed depression was actually due to a conductance decrease. The conductance was evaluated by a short negative voltage pulse applied when the C current was fully developed (Fig. 8B). The delayed depression induced by a short conditioning pulse was paralleled by a decrease in the current jump induced by the negative pulse.

The delayed blocking effect induced by a short depolarizing pulse was specific to the C current. In the experiment illustrated in Fig. 8Ci, the compound outward current elicited in response to a test pulse at +80 mV was determined in a P cell bathed in the standard $Na^+$-free saline. A short conditioning pulse (+20 mV, 30 ms) induced a delayed blockade of part of the outward current (Fig. 8Di).

The cell was then injected with EGTA and the sequence was repeated. The

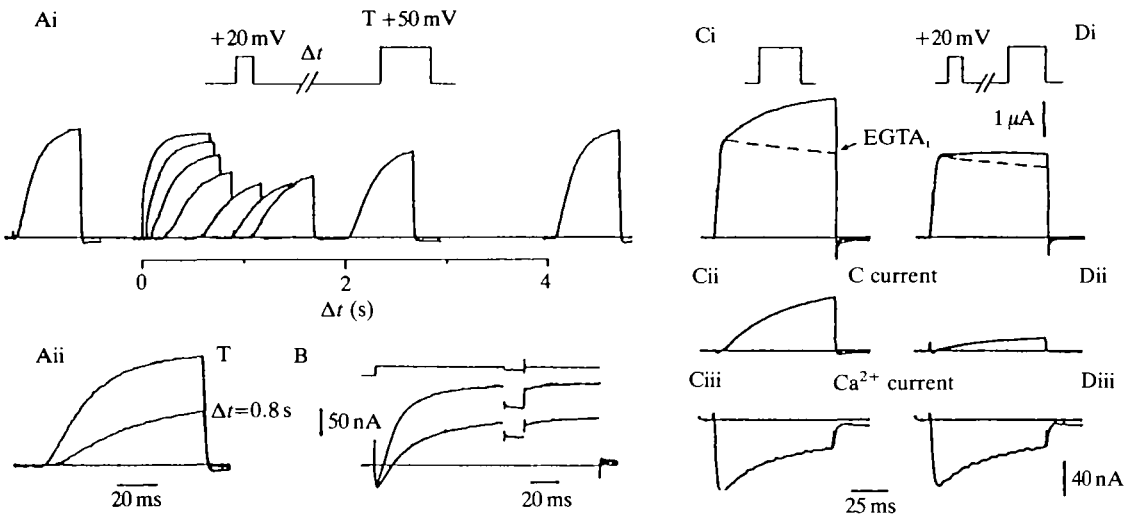


Fig. 8. Delayed blockade of C current. (A) $TEA^+$-injected P cell; $TEA^+$-resistant current subtracted. C current induced by a +50 mV test pulse (T) applied at various intervals ($\Delta t$) after a short conditioning pulse: +20 mV, 50 ms. Left-hand recording in Ai, control slow C current without conditioning pulse. Superimposed current traces are arranged according to the interpulse interval (from left to right, 25 ms to 4 s) showing early facilitation, late depression (0.5–0.8 s interval) and slow recovery following the conditioning pulse. Control and depressed currents ($\Delta t$=0.8 s) are shown in Aii. (B) The late depression of the outward current was due to a conductance decrease. Same conditions as in Aii. The conductance was evaluated from the current jump induced by a short 10 mV negative pulse superimposed on the test pulse. (Ci) Current induced by a test pulse (+80 mV), before (solid line) and after EGTA injection ($EGTA_i$) (dashed line). (Cii) C current suppressed by intracellular EGTA. (Ciii) The cell was then bathed in the 60 mmol $l^{-1}$ $TEA^+$ $Na^+$-free saline and the test pulse was set at +10 mV in order to produce a large $Ca^{2+}$ current. (D) Same series as in C with the test pulse applied 0.7 s after a conditioning pulse (+20 mV, 50 ms).

voltage-dependent outward current is indicated by the dashed lines in the total outward current in Fig. 8Ci,Di. The C current under the two experimental conditions is shown in Fig. 8Cii,Dii. The cell was then bathed in the $TEA^+$-saline and the test pulse was set at +10 mV in order to observe the $Ca^{2+}$ current (Fig. 8Ciii,Diii). This experiment shows that the short conditioning pulse had a delayed depressing effect only on the C current. In particular, the $Ca^{2+}$ current in the test pulse was not significantly altered by the conditioning pulse. When the EGTA injection was omitted, short (20–30 ms) conditioning depolarizations had weak blocking effects on $Ca^{2+}$ currents (less than 10 % reduction in the test $Ca^{2+}$ current), which ruled out the hypothesis that calcium current inactivation caused the C current blockade.

The amount of blockade depended neither on the test pulse level (ranging from −30 to +120 mV) nor on the inter-pulse potential (from −40 to −100 mV). It was directly related to the conditioning pulse level. In the experiment shown in Fig. 9,

a $TEA^+$-injected cell was given a test pulse (−10 mV, 80 ms) 0.7 s after a short conditioning pulse of variable amplitude. Blockade of the C current was induced by conditioning depolarizations at levels more positive than −30 mV. The blockade first increased with the conditioning potential amplitude (Fig. 9Ai), and then decreased when the conditioning pulse was large (Fig. 9Aii). Maximum blockade occurred with conditioning potentials between 0 and +30 mV. The current suppressed by the conditioning pulse (series B of Fig. 9) had the slow sigmoidal onset characteristic of the C current. The plot of this current against the conditioning potential level (Fig. 9C) showed that maximum blockade occurred at +10 mV and that it vanished at large depolarizations, with an extrapolated null-current potential of nearly +100 mV.

A similar dependence on potential applied to the pulse-induced facilitation of

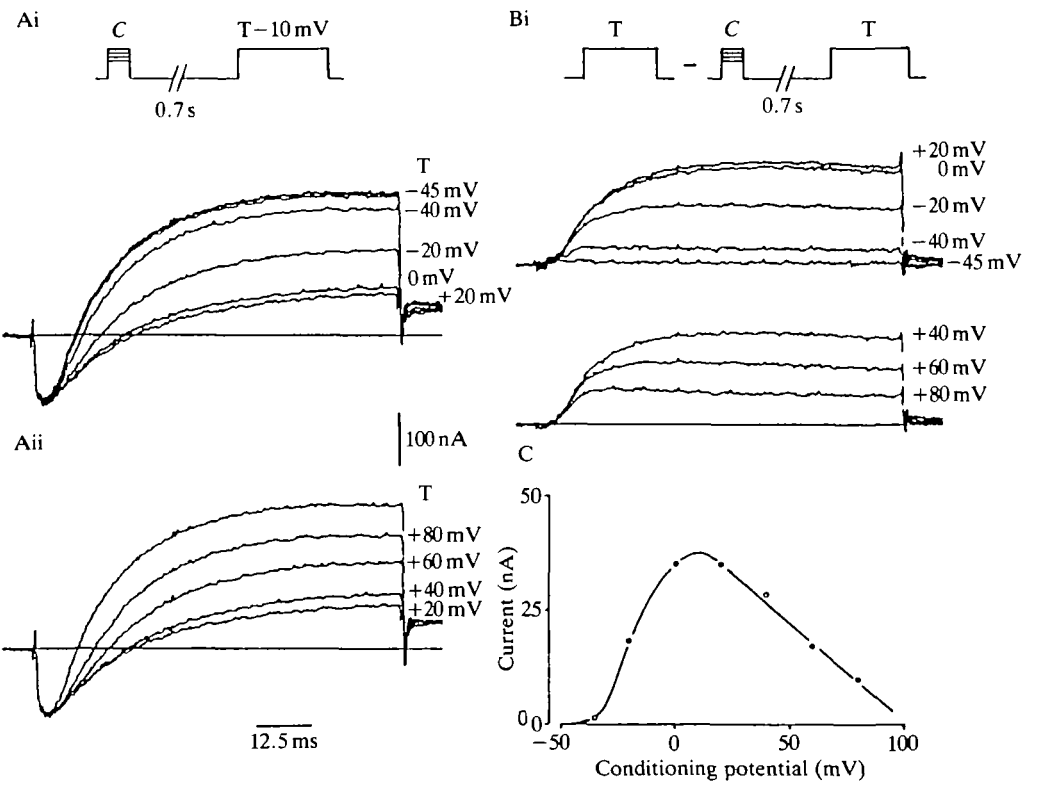


Fig. 9. $Ca^{2+}$-induced delayed blockade of C current. The delayed blockade of the C current was related to the size of the $Ca^{2+}$ current in the conditioning pulse. $TEA^+$-injected P cell. Test pulse: −10 mV. Conditioning pulse (*c*) (30 ms duration) applied 0.7 s before the test pulse. Conditioning potential level indicated on current traces together with the control test current (T). Increasing the conditioning pulse amplitude first reduced (Ai) then increased (Aii) the outward current, with no appreciable change in the peak $Ca^{2+}$ current. Series Bii (obtained from corresponding recordings in series A) shows the current suppressed by the conditioning pulse. The data are displayed in C.

the C current (see Fig. 6) and to its activation time course (see Fig. 5); both phenomena were related to the size of the $Ca^{2+}$ current. It was therefore likely that the C current blockade was induced, after a latency of 0.5–1 s, by intracellular $Ca^{2+}$ accumulation. If this hypothesis is correct, it remains to be explained how long-lasting (5–10 s) depolarizations of reduced amplitude (less than 20 mV depolarization from the −50 mV holding potential) were able to suppress the C current fully.

Both inactivating procedures (long-lasting moderate depolarization or short large pulses) affected the C current similarly. This is illustrated in Fig. 10A. In a

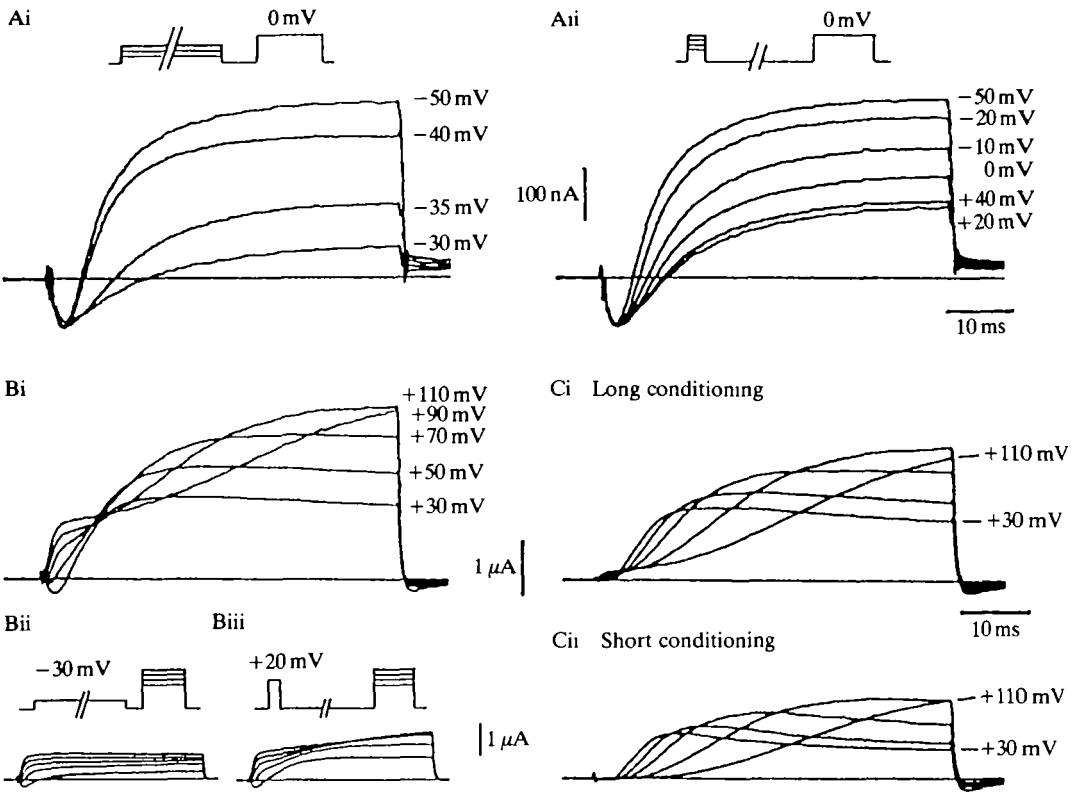


Fig. 10. Evaluation of the C current blockade induced by a short $Ca^{2+}$ entry. (A) $TEA^+$-injected P cell. Superimposed currents in response to a test pulse to 0 mV. C current inactivation induced by 10 s depolarization (Ai) or by a short (30 ms) conditioning pulse applied 0.8 s before the test pulse (Aii). Conditioning levels are indicated on current traces. The C current blockade was not paralleled by any decrease in inward $Ca^{2+}$ current. The outward current that persisted after 10 s of conditioning at −30 mV was the $TEA^+$-resistant voltage-gated $K^+$ current. (B) $TEA^+$-injected P cell subjected to various test pulses at the levels indicated in Bi. (Bii, Biii) Test pulses applied either immediately after a 10 s conditioning depolarization at −30 mV (Bii) or 0.8 s after a 30 ms depolarization at +20 mV (Biii). The currents suppressed by either conditioning programme are displayed in Ci and Cii, respectively. In A and B, the C current was blocked by 60–70 % after a short early $Ca^{2+}$ entry.

$TEA^+$-injected P cell, a test pulse (10 mV, 80 ms) was delivered either 0.1 s after a long-lasting (10 s) depolarization of moderate amplitude (Fig. 10Ai) or 0.7 s after a short (30 ms) depolarizing pulse (Fig. 10Aii). Test current blockade was induced in both cases by progressively increasing the conditioning pulse amplitude. The same blockade was observed with a long conditioning pulse at −35 mV and with a short depolarization at +20 mV. The $TEA^+$-insensitive voltage-gated $K^+$ current was not appreciably affected. It corresponded to the outward current remaining after long conditioning at −30 mV in Fig. 10A.

Series B and C in Fig. 10 were from another $TEA^+$-injected P cell subjected to test pulses of increasing amplitude. Fig. 10Bi–Biii shows sets of control currents (Bi) and currents persisting after conditioning depolarizations at −30 mV for 10 s (Bii) or at +20 mV for 30 ms (Biii). The currents suppressed by these two inactivating programmes are displayed in Fig. 10Ci and 10Cii, respectively, and clearly show that both inactivating processes affected the outward current similarly. The amount of blockade induced by the short conditioning pulse was 63 % of that induced by the long conditioning depolarization; it was not dependent on the level of the test pulse.

Inactivation of the C current could thus be induced by using three different voltage programmes: (a) during prolonged depolarizations; (b) in response (delayed by 0.5–1 s) to a short depolarizing pulse; (c) following a long-lasting conditioning depolarization between −30 and −40 mV.

Data from programmes a and b suggested a $Ca^{2+}$-induced blockade of the C current. In both cases, the amount of blockade was directly related to the size of the $Ca^{2+}$ current. The $Ca^{2+}$ current in P cells had a consistent activation with potentials of more than −30 mV and a peak value at about +20 mV (see Fig. 5). The blockade resulting from moderate depolarizations in the −30 to −40 mV range therefore did not seem to be attributable to intracellular $Ca^{2+}$ accumulation. This question was re-examined in experiments designed to detect very small $Ca^{2+}$ currents in the negative voltage range. Several studies have shown the existence of slow inward currents, probably carried by calcium ions, which are detectable at voltages as low as −40 mV or even below (Eckert and Lux, 1976; Gorman *et al.* 1982; Adams and Levitan, 1985). Slow currents of this kind have been detected in pacemaker bursting neurones in *Helix* and *Aplysia* (Adams and Levitan, 1985).

EGTA was injected into a P cell. The C current was identified as the EGTA-sensitive current. The cell was then bathed in the 60 mmol $l^{-1}$ $TEA^+$, $Na^+$-free saline, and subsequently in the same saline in which $Co^{2+}$ was substituted for $Ca^{2+}$. The $Ca^{2+}$ current was identified with the current suppressed by $Co^{2+}$ (current in the $TEA^+$–$Ca^{2+}$ saline minus current in the $TEA^+$–$Co^{2+}$ saline). With this subtraction method, it was possible to detect minute $Ca^{2+}$ currents. Results on the C and $Ca^{2+}$ currents in the same P cell are shown in Fig. 11.

The $Ca^{2+}$ current had a detectable threshold at −40 mV. Its peak level increased slightly with the potential in the range of −40 to −30 mV; steeper increases with voltage were then observed. The C current had an activation threshold at −25 mV

These findings showed: (1) that inactivation of the C current can be induced

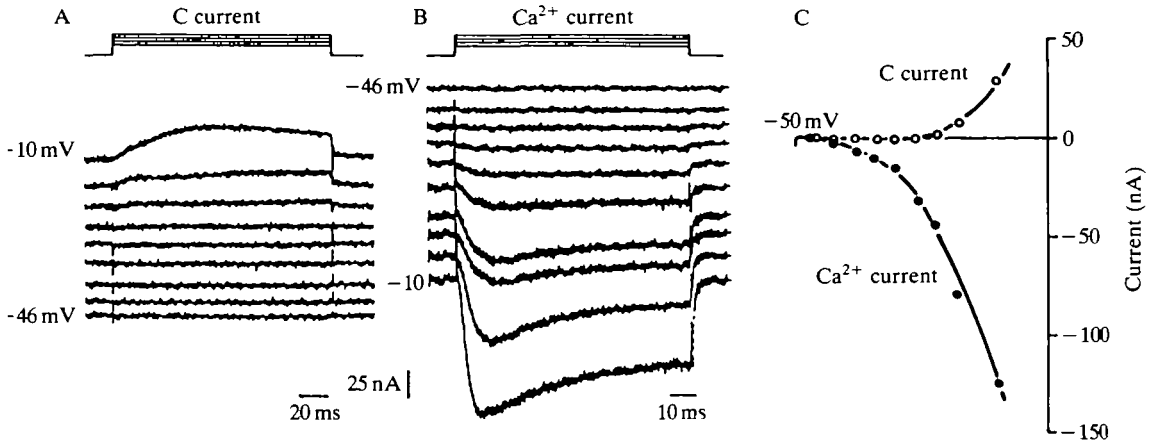


Fig. 11. $Ca^{2+}$ and C current activation threshold. $TEA^{+}$-injected P cell depolarized at the levels indicated (voltage changed in 4 mV steps). Holding potential: −50 mV. C and $Ca^{2+}$ currents were isolated successively by intracellular injection of EGTA (C current) and by substituting $Co^{2+}$ (8 mmol $l^{-1}$) for $Ca^{2+}$ ($Ca^{2+}$ current). (C) Peak current *versus* membrane potential. The $Ca^{2+}$ current has a detectable voltage threshold at −40 mV and a maximum value of 220 nA at +20 mV (off scale). The threshold for C current activation was −25 mV.

from its resting state (inactivation from the activated state occurred in the above stimulation programme a); and (2) that moderate long-lasting depolarizations in the −30 to −40 mV range induce $Ca^{2+}$ currents that can result in intracellular $Ca^{2+}$ accumulation. These $Ca^{2+}$ currents were nevertheless tiny, which accounts for the slow time course of the C current inactivation process: the time constants of the inactivation induced by long-lasting depolarizations were 3 s at −40 mV and 1.5 s at −30 mV.

The kinetic data from the three different inactivating programmes were therefore in agreement with the $Ca^{2+}$-induced blockade hypothesis. The possibility could not be ruled out, however, that, with long-lasting conditioning depolarizations (programme c), the blockade might be a voltage-dependent process directly induced by the cell depolarization and not by the resulting $Ca^{2+}$ entry.

### *Intracellular $Ca^{2+}$ injections*

$Ca^{2+}$ injections were performed either by pressure or ionophoretically. In both cases, the pipettes used were of the patch-clamp type (see Materials and methods) with a tip diameter of about 1 μm. Pipettes for pressure injection were filled with 0.1 mol $l^{-1}$ $CaCl_2$ in 0.1 mol $l^{-1}$ KCl. Pipettes for ionophoretic injections were filled with 10–50 mmol $l^{-1}$ $CaCl_2$ in distilled water. Higher concentrations led to frequent blockade when ejecting current was applied.

Effective $Ca^{2+}$ injections with pressure ($1\times10^{5}$–$2\times10^{5}$ Pa for 0.5–5 s) were

signalled by a transient inward current when the cell was at the −50 mV holding potential (Hofmeier and Lux, 1981). $Ca^{2+}$ ejections were greatly improved by applying a retention current to the $Ca^{2+}$-filled electrode. The data given in Fig. 12A were obtained from a $TEA^+$-injected P cell. Holding current and current induced by a short pulse (+70 mV, 80 ms) are displayed at two different magnifications in Fig. 12Ai and 12Aii. The current trace in Fig. 12Aii also shows current jumps induced by 40 mV, 2 s hyperpolarizing pulses. Two successive $0.5\times10^5$ Pa, 3 s pressure pulses were applied to the $Ca^{2+}$-filled electrode. A 10 nA retention current was injected just before the second trial, using the method described by Hofmeier and Lux (1981). No effect was observed with the first trial, whereas the second trial produced an immediate inward current, a delayed increase in membrane conductance (increase in the current jump in response to the 40 mV hyperpolarizing pulse) and a decrease in the outward current triggered by the +70 mV pulse. The outward current recovery to the control level was over

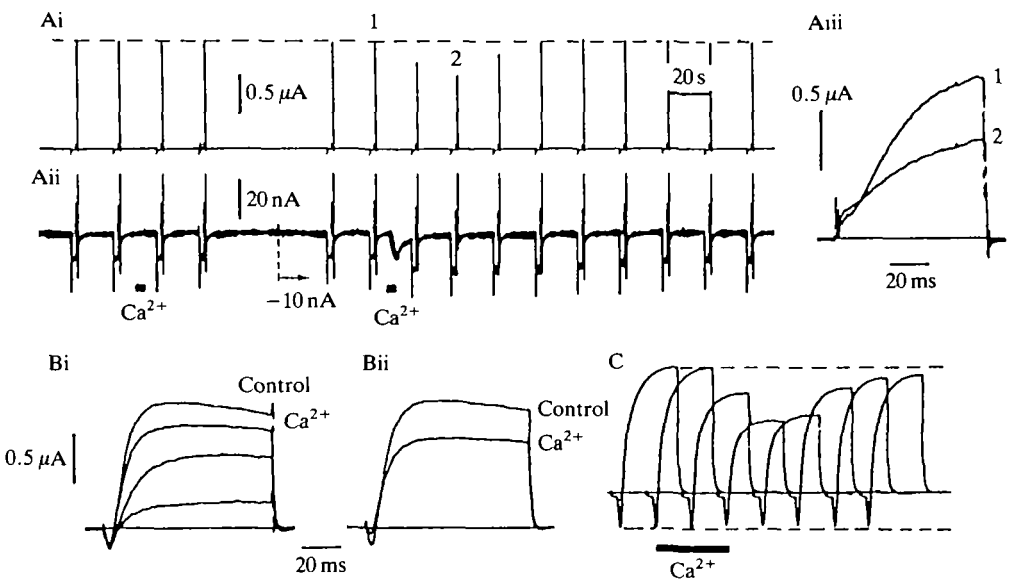


Fig. 12. C current blockade induced by intracellular $Ca^{2+}$ injection. (A) Continuous recording of currents induced by depolarizing pulses to +70 mV (Ai) and by 40 mV amplitude hyperpolarizing pulses (Aii) in a $TEA^+$-injected P cell. Black bars: pressure ($0.5\times10^5$ Pa, 3 s). A permanent 10 nA inward current was passed through the $Ca^{2+}$-filled electrode before the second trial. Successful $Ca^{2+}$ injection produced an immediate inward current and a delayed increase in membrane conductance. Concomitantly the outward current induced at +70 mV was partly blocked. Recordings labelled 1 and 2 are displayed in Aiii. (B) $TEA^+$-injected P cell. $Ca^{2+}$ pressure-injected. (Bi) $10^5$ Pa, 3 s. (Bii) $10^5$ Pa, 5 s. (Bi) Currents in response to a +10 mV pulse. From top to bottom: control; 10 s after $Ca^{2+}$ injection; current partly blocked by a +20 mV, 30 ms pulse applied 0.7 s before; current fully blocked by 10 s conditioning at −30 mV. (Bii) Control and after $Ca^{2+}$ injection. (C) Ionophoretic injection of calcium. $TEA^+$-injected P cell, ionophoretic current: 50 nA, 40 s. Successive recordings (test pulse 0 mV) performed every 20 s.

in less than 1 min, but the resting membrane conductance took longer (5–10 min) to recover. Details in Fig. 12Aiii show the prominent decrease in the slow C current component induced by $Ca^{2+}$ injection.

Although $Ca^{2+}$ injections mimicked the delayed blocking effect resulting from a short $Ca^{2+}$ entry, they proved to be less effective. The data given in Fig. 12Bi were obtained from a $TEA^{+}$-injected P cell, pulse-depolarized at +30 mV. The C current was decreased by 25 % after a 3 s $Ca^{2+}$ injection ($1\times10^{5}$ Pa) and by 50 % after a $Ca^{2+}$ entry produced by a short pulse (+20 mV, 50 ms). In neither case was any change in the inward $Ca^{2+}$ current observed.

When the duration of $Ca^{2+}$ injection was increased (Fig. 12Bii), the C current blockade was larger but it was paralleled by a decrease in the peak $Ca^{2+}$ current. It was not clear, however, whether this decrease was actually attributable to a $Ca^{2+}$-induced $Ca^{2+}$ current blockade. Part of this decrease was presumably attributable to shunting by the increased leakage current (Hofmeier and Lux, 1981). During the first minute of recovery, the C current reached its control level while the peak $Ca^{2+}$ current was still depressed. The peak $Ca^{2+}$ current then recovered, together with the resting conductance. Since we always observed a more or less direct relationship between the magnitude of C and $Ca^{2+}$ currents, the recovery of the C current would have to be paralleled by that of the $Ca^{2+}$ current.

Ionophoretic injections of calcium yielded similar results, except that we did not observe any fast $Ca^{2+}$-induced inward current and the increase in the resting conductance was less pronounced than after pressure injections. Nevertheless, large injections (50–100 nA ionophoretic current for 2–4 min) also increased the leakage current, which obscured possible changes that could affect the $Ca^{2+}$ current. Moderate $Ca^{2+}$ injections (30–50 nA, 30–60 s) produced a clear C current blockade with little or no change in the peak $Ca^{2+}$ current, as shown in Fig. 12C, where the C current was half blocked by a 40 s $Ca^{2+}$-injection with 50 nA.

Moderate $Ca^{2+}$ injections (with either pressure or current) that proved effective in partly blocking the C current had apparently no effect on its activation time course; the depressed C current had the same slow sigmoidal onset as the test current, i.e. it showed no sign of any facilitated activation attributable to a large intracellular $Ca^{2+}$ accumulation. The depressed C current, however, switched to the fast-activating mode when it immediately followed a short depolarizing pulse (+20 mV, 30 ms; not illustrated). These results suggest that the increase in intracellular calcium concentration produced by pressure or ionophoretic injection was not large enough to accelerate the C current, whereas it effectively reduced its peak level.

## Discussion

In our preceding paper (Pin *et al.* 1990), we showed that a nerve cell group in *Helix* generates long-lasting plateaus sustained by a persistent $Ca^{2+}$ current. The depolarized plateau appears suddenly after a firing period at low frequency (5 Hz) during which the spikes progressively enlarge. The aim of the present paper was to

determine the properties of the repolarizing currents which might account for the transition from firing to plateau. It emerges that the plateau-generating cells (P cells) do not differ much in this respect from most other *Helix* neurones, in which calcium ions make a significant contribution to the depolarizing inward current. For instance, the large nerve cells, referred to as A cells in our previous paper, have $Ca^{2+}$ and $K^+$ currents in the same proportion as in P cells; they nevertheless do not produce plateaus or long-lasting spikes. Therefore, P cells do not appear to be intrinsically devoid of repolarizing currents. These findings led us to examine more closely the properties of the $K^+$ currents in order to determine why these currents could not effectively counteract the depolarizing tendency of the $Ca^{2+}$ current.

### *Voltage-gated $K^+$ currents*

Two $K^+$ currents contribute to the delayed outward current in P cells: a voltage-gated $K^+$ current and a $Ca^{2+}$-activated $K^+$ current. Voltage-gated $K^+$ currents in molluscan nerve cells display a variable degree of relaxation under sustained depolarization. It has already been observed that the relaxation may differ from cell to cell (Magura *et al.* 1971; Thompson, 1980; Aldrich, 1981). This is also the case in *Helix* neurones, in which P cells and a few other neurones (such as A cells) have a prominent inactivating process. This inactivating process was routinely estimated from the relative amount of relaxation in 0.7–0.8 s depolarizations at +30 to +50 mV. In a wide variety of cells, relaxation ratios ranging from 0.24 to 0.7 were obtained. P and A cells have the largest inactivating ratio, whereas bursting cells are characterized by moderate inactivation (0.30–0.35). These findings strongly suggest that two different K(V) currents, with or without inactivation, contribute variably to the delayed rectifying current. No differences could be detected, however, between the activating processes in these cells: K(V) currents with either large or moderate inactivation have identical activation–voltage curves and activation kinetics. Similarly, the steady-state inactivation–voltage curve was found to be identical in all cells. The non-inactivating K(V) current (which persisted after 10 s of depolarization) was also found to be unrelated to the inactivating ratio as defined previously. Therefore, the main difference between these cells lies in the speed of the inactivating process rather than in its magnitude. Cells such as P cells have a fast inactivating process, whereas bursting cells have a slow one. It is nevertheless worth noting that, in both cell types, inactivation is a well-characterized voltage-dependent process with identical steady-state properties. A possible explanation for the variability of the inactivating rate is based on the data from Ruben and Thompson (1984). These authors have suggested that inactivation might be induced by an intracellular removable blocker which might interact with the open channel in a voltage-dependent manner. The speed with which the blocker acts might be directly dependent on its local concentration, whereas the steady-state amount of blockade might reflect the voltage-dependency of the channel–blocker interaction. This hypothesis is attractive to the extent that a mechanism of this kind would give cells additional adaptive

capacities involving the regulation of the number of active channels rather than that of their gating characteristics.

### *$Ca^{2+}$-activated $K^+$ currents*

The $Ca^{2+}$-dependent $K^+$ component in P cells has the same main properties as the C current originally identified in *Helix* neurones by Meech and Standen (1975). This current has an activation threshold at −30 mV, a peak amplitude at +20 to +50 mV and it vanishes when the potential approaches the equilibrium potential for calcium ions (over +100 mV) (see reviews by Meech, 1978; Schwarz and Passow, 1983; Rudy, 1988).

The C current in P cells was very sensitive to extracellular $TEA^+$ ($K_d \approx$ 1 mmol $l^{-1}$) and insensitive to intracellular $TEA^+$, extracellular 4-AP and apamin. These properties are identical to those of the $K^+$ current induced by $Ca^{2+}$ injections in molluscan neurones (Hermann and Gorman, 1981; Onozuka *et al.* 1988). These results differ from those published by other workers (Heyer and Lux, 1976; Thompson, 1977; Kostyuk *et al.* 1980), who suggest that the $Ca^{2+}$-activated $K^+$ current is $TEA^+$-insensitive. This discrepancy may be due merely to the experimental techniques employed and the criteria used to identify the $Ca^{2+}$-activated current component.

The properties of the C current in *Helix* nerve cells have been described in detail by Lux and Hofmeier (1982*a*,*b*) and by Gola *et al.* (1990). These authors made use of a nerve cell group (U cells) in which the outward current flows almost solely in C channels. In U cells as well as in P cells, the C current is characterized by a dramatic slowing down at large positive potentials. This phenomenon has been attributed to a peculiar voltage-dependency of the gating process (Lux and Hofmeier, 1982*b*). The following data suggest that the C current activation time course in P cells is actually rate-limited by the intracellular $Ca^{2+}$ concentration. (1) The time to half-activation had a minimum value at potential levels that produced large $Ca^{2+}$ entries. (2) This time was altered in a $Ca^{2+}$-dependent manner when $Ca^{2+}$ currents were manipulated through changes in the $Ca^{2+}$ content of the saline. (3) Increasing the $Ca^{2+}$ entry by means of appropriate short depolarizations speeded up the C current onset.

All these data are in agreement with the idea that a rate-limiting role may be played by calcium on C current activation. It follows that, in potential ranges producing large inward $Ca^{2+}$ currents, the C current may have a fast onset (half-activation in 6–8 ms). Therefore, the C current in P cells has ideal properties for exerting powerful repolarizing effects. The involvement of the C current in the repolarization of $Ca^{2+}$-dependent spikes in *Helix* U cells has already been demonstrated (Gola *et al.* 1986, 1989).

### *$Ca^{2+}$-induced C current blockade*

High intracellular calcium levels can block a variety of channels. The first reported example was that of calcium channels which are inactivated by processes depending either on voltage or on intracellular calcium (or on both). Several

potassium channels have been reported to be inactivated by elevated $[Ca^{2+}]_i$: delayed outward channels in *Helix* neurones (Heyer and Lux, 1976; Eckert and Lux, 1977), T lymphocytes (Bregestovski *et al.* 1986) and photoreceptors (Chinn and Lisman, 1984; Alkon *et al.* 1984), inward rectifiers in *Aplysia* neurones (Kramer and Levitan, 1988), M channels in sympathetic ganglia (Tokimasa, 1985), fast A channels in molluscan neurones (Thompson, 1977), rat sympathetic neurones (Galvan and Sedlmeier, 1984), mammalian central neurones (Gustafsson *et al.* 1982) and bullfrog ganglion cells (Brown *et al.* 1982) and ATP-sensitive $K^+$ channels in myocytes (Findlay, 1988). Some $Ca^{2+}$-activated $K^+$ channels may also be blocked by $[Ca^{2+}]_i$ (Vergara and Latorre, 1983; Onozuka *et al.* 1988).

In *Helix* P cells, the C current inactivation is induced by three different voltage programmes: (a) during a long-lasting (0.7–0.8 s) depolarization; (b) 0.5–1 s after a short calcium entry; (c) after a 5–10 s conditioning depolarization between −30 and −40 mV. The threshold of C current activation is about −30 mV. Therefore, blockade of the C current could be induced both from the activated state (programme a) and from the resting state (programmes b and c).

In the above three situations, inactivation proceeds at a rather slow rate. Following a short large $Ca^{2+}$ entry (programme b), maximum blockade is observed 0.5–1 s later. This delayed blocking effect on $K^+$ currents was first observed in *Helix* neurones by Eckert and Lux (1977). With short inter-pulse intervals in programme b (<0.1 s), the C current has the fast onset ascribed to the $Ca^{2+}$-induced facilitating effect reported in the preceding section. As the interpulse interval increases, the facilitation (evaluated from the activation rate) progressively vanishes, while the peak C current decreases. The depressed C current (30–40 % of the control level) no longer shows any sign of facilitated onset but an additional $Ca^{2+}$ entry, occurring just before the test pulse accelerates the depressed C current. These data strongly suggest that inactivation, in comparison with activation, is a very sensitive $Ca^{2+}$-dependent process.

Since $Ca^{2+}$ entry is required for C channels to be opened by cell depolarization, the block which followed a short conditioning pulse might result from voltage- and/or $Ca^{2+}$-induced inactivation of $Ca^{2+}$ channels (Chad *et al.* 1984). This hypothesis has been put forward by Eckert *et al.* (1981) to account for the decrease in $Ca^{2+}$-activated $K^+$ currents in *Helix* bursting neurones. The loss of C current in internally perfused *Helix* neurones has also been ascribed to a $Ca^{2+}$ channel blockade by elevated $[Ca^{2+}]_i$ (Levitan and Levitan, 1986). This does not appear to be the case in P cells: the C current blockade occurred in the absence of any detectable $Ca^{2+}$ current decrease. A $Ca^{2+}$-induced inactivation of $Ca^{2+}$ channels also occurs in P cells but requires longer and larger inactivating prepulses to be observed, which confirms that the C current inactivating process has a very high affinity for calcium.

Evidence that C channels are blocked by accumulated intracellular calcium and not by voltage is provided by the bell-shaped relationship that exists between the level of the short inactivating pulse and the amount of C current blockade (voltage programme b). This curve has a peak at about +20 mV, which is a characteristic of

membrane processes that are caused by $Ca^{2+}$ influx, such as activation of C current (Meech and Standen, 1975) and inactivation of voltage-gated $Ca^{2+}$ current (Eckert *et al.* 1981). The usual way to test $Ca^{2+}$ involvement in a given process is to clamp the intracellular free $Ca^{2+}$ with a $Ca^{2+}$ chelator. This test could not be performed, however, since $Ca^{2+}$ accumulation is required for the C current to be activated. Therefore, instead of preventing the C current blockade we attempted to induce blockade with intracellularly injected calcium ions. Injection with either pressure or current yielded comparable results. Specific blockade of the C current was obtained with moderate $Ca^{2+}$ injections. The block was nevertheless of limited amplitude (about 50 %). Larger $Ca^{2+}$ injections led to persistent increases in cell membrane conductance (see Hofmeier and Lux, 1981) which obscured the changes in C and $Ca^{2+}$ currents.

Inactivation induced by long-lasting conditioning between −30 and −40 mV confirms that the inactivating process is very sensitive to calcium. In this potential range, very tiny $Ca^{2+}$ currents are produced. At −35 mV, a level producing half-blockade of the C current, the peak $Ca^{2+}$ current is only a few nanoamps, about 2–3 % of the $Ca^{2+}$ current available at +20 mV. Such a tiny $Ca^{2+}$ entry has no effect on the $Ca^{2+}$ current itself and on the activation rate of the C current.

Examination of the effects of $Ca^{2+}$ entry on C and $Ca^{2+}$ currents yields the following order in terms of $Ca^{2+}$ sensitivity: C current inactivation>$Ca^{2+}$ current inactivation>C current activation. The same sequence was deduced from the effects of intracellular $Ca^{2+}$ injections. Moderate injections selectively inactivated C channels; larger injections were necessary to inactivate $Ca^{2+}$ channels. In both cases, the time course of C current activation, which was considered to be an index of the submembrane free calcium level, remained unaltered.

Blockade of $Ca^{2+}$-activated $K^+$ channels by $[Ca^{2+}]_i$ has been described in muscle cells (Vergara and Latorre, 1983), in pig pancreatic acinar cells (Iwatsuki and Petersen, 1985), in bovine parathyroid cells (Jia *et al.* 1988) and in molluscan nerve cells (Onozuka *et al.* 1988). Although large variations in the dependence on $[Ca^{2+}]_i$ were observed, the closing process had a lower affinity for calcium than the opening process. Our data suggest that the C channel in *Helix* P cells has a receptor for the closing process that has a higher affinity for calcium than has the opening process. It follows that the channels would stay closed at either reduced or elevated $[Ca^{2+}]_i$ and that they could be opened only transiently upon fast $[Ca^{2+}]_i$ increase.

Additional evidence of highly sensitive $Ca^{2+}$-dependent inactivation is provided by the time course of recovery from inactivation following a brief $Ca^{2+}$ entry. Recovery is a slow process, independent of cell potential and inactivating procedure. The mean time constant of recovery is 3.4 s, a figure close to that of the $[Ca^{2+}]_i$ recovery (5 s) monitored using the $Ca^{2+}$-sensitive dye Arsenazo III in *Aplysia* neurones (Thomas and Gorman, 1977). Since resting $[Ca^{2+}]_i$ in *Helix* nerve cells is below 0.1 $\mu$mol $l^{-1}$ (Alvarez-Leefman *et al.* 1981; Hofmeier and Lux, 1981), C channel blockade might be induced by submicromolar increases in $[Ca^{2+}]_i$. Therefore, $Ca^{2+}$ entry during firing might induce C channel blockade

(after a 0.5–1 s latency). Additional $Ca^{2+}$ entry produced by successive spikes might fail to open inactivated C channels, since inactivation prevails over activation. This would result in spike lengthening, which in turn would favour the voltage-dependent blockade of K(V) channels. The process would continue to the point where depressed outward currents are overtaken by the $Ca^{2+}$ current, which would result in long-lasting depolarizations at a positive potential level.

None of the ionic currents involved in the spike–plateau pattern in P cells appears to have unusual properties. $Ca^{2+}$ currents have similar gating properties and amplitudes to those commonly found in a number of other identifiable *Helix* neurones. Voltage-gated and $Ca^{2+}$-activated $K^+$ currents also have gating properties in common with neurones in which calcium ions contribute to the spike production. Inactivation of both $K^+$ currents is also commonly observed in several nerve cells, although cells such as U cells have a non-inactivating C current (Lux and Hofmeier, 1982*a*). In contrast to the well-characterized activating processes, however, inactivation displays a large range of individual variations.

Data collected in the four nerve cell types (P, A, bursting and U cells) are summarized in Fig. 13. These cells were selected because they have $Ca^{2+}$ currents that can produce spikes when bathed in $Na^+$-free salines. P and A cells are characterized by pronounced $K^+$ current inactivating processes (Fig. 13C); they have almost identical $Ca^{2+}$ currents (measured at +20 mV, Fig. 13B). The fact that A cells do not display long-lasting spikes and plateaus is probably due to their relatively high density of $K^+$ channels, almost twice that in P cells (Fig. 13A). Although inactivated by 70–80 % by prolonged depolarization, the remaining $K^+$ current in A cells is still able to repolarize the spike. Bursting Br cells have a $K^+$ channel/$Ca^{2+}$ channel ratio similar to that found in P cells. The moderate voltage-

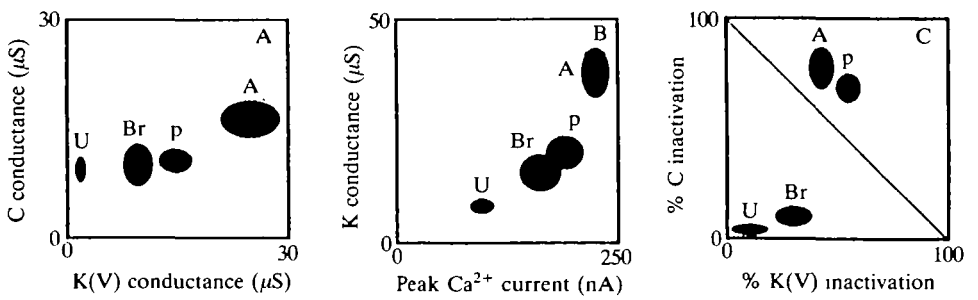


Fig. 13. A diagram of the properties of the U, Br, P and A neurones. (A) C conductance/K(V) conductance ratio. The C current amounts to 36 % of the total $K^+$ current in A cells, 40 % in P cells and 97 % in U cells. (B) $K^+$ conductance/$Ca^{2+}$ current ratio. The $K^+$ conductance is the sum of the K(V) and C conductances. The $Ca^{2+}$ current was measured at its peak amplitude (between +10 and +30 mV). (C) Plot of the inactivation of the K(V) and C currents. The percentage of inactivation was measured after 800 ms of depolarization at +20 to +50 mV. A and P cells are located in the part where inactivation reduces the total $K^+$ current by more than 50 %. In all three diagrams, black surfaces correspond to mean values±S.D. ($N$=5–16).

and $Ca^{2+}$-induced inactivation in these cells prevents extensive spike broadening during firing. This safety mechanism is primarily played by C channels since it has been demonstrated that $Ca^{2+}$ accumulation during firing speeds up the non-inactivating C current in U cells (Gola *et al.* 1986), which may stop the firing (Chagneux *et al.* 1989). Therefore, the unusual firing properties of P cells arise both from the quantitative adjustment of depolarizing and repolarizing currents and from the existence of regulatory mechanisms that affect simultaneously the voltage-gated and the $Ca^{2+}$-gated $K^+$ channels.

The main result of this study is the finding that widely distributed potassium channels with apparently identical gating characteristics are subjected to regulatory processes. These processes do not affect their gating mechanisms but they alter the number of available channels in a manner that is specific to the cell under consideration. It is tempting to suggest that these regulations are either linked to cellular metabolic processes or are under the control of extracellular messengers or both. To elucidate them would give new insights into the mechanisms underlying the modulation of nerve cell signalling.

We are grateful to Dr K. Kits (Vrije Universiteit, Biologisch Laboratory, Amsterdam) for his critical comments on an earlier version of the manuscripts which led to their improvement.

## References

ADAMS, W. B. AND LEVITAN, I. B. (1985). Voltage and ion dependences of the slow currents which mediate bursting in *Aplysia* neurone R15. *J. Physiol., Lond.* **360**, 69–93.

ALDRICH, R. W. (1981). Inactivation of voltage-gated delayed potassium current in molluscan neurons. A kinetic model. *Biophys. J.* **36**, 519–532.

ALDRICH, R. W., GETTING, P. A. AND THOMPSON, S. H. (1979). Mechanism of frequency dependent broadening of molluscan neurone soma spike. *J. Physiol., Lond.* **291**, 531–544.

ALKON, D. L., SHOUKIMAS, J. J. AND HELDMAN, E. (1984). Calcium-mediated decrease of a voltage-dependent potassium current. *Biophys. J.* **40**, 245–250.

ALVAREZ-LEEFMANS, F. J., RINK, T. J. AND TSIEN, R. Y. (1981). Free calcium ions in neurones of *Helix aspersa* measured with ion selective micro-electrodes. *J. Physiol., Lond.* **315**, 531–548.

BREGESTOVSKI, P., REDKOSUBOV, A. AND ALEXEEV, A. (1986). Elevation of intracellular calcium reduces voltage-dependent potassium conductance in human T cells. *Nature* **319**, 776–778.

BROWN, D. A., CONSTANTI, A. AND ADAMS, P. R. (1982). Calcium-dependence of a component of transient outward current in bullfrog ganglion cells. *Neurosci. Abstr.* **8**, 252.

CHAD, J. E., ECKERT, R. AND EWALD, D. (1984). Kinetics of calcium dependent inactivation of calcium current in voltage-clamped neurones of *Aplysia californica*. *J. Physiol., Lond.* **347**, 279–300.

CHAGNEUX, H., DUCREUX, C. AND GOLA, M. (1989). Voltage-dependent opening of single calcium-activated potassium channels in *Helix* neurons. *Brain Res.* **488**, 336–340.

CHINN, K. AND LISMAN, J. (1984). Calcium mediates the light-induced decrease in maintained K current in *Limulus* photoreceptors. *J. gen. Physiol.* **84**, 447–462.

CONNOR, J. A. AND STEVENS, C. F. (1971). Inward and delayed outward membrane currents in isolated neural somata under voltage clamp. *J. Physiol., Lond.* **213**, 1–19.

ECKERT, R. AND LUX, H. D. (1976). A voltage-sensitive persistent calcium conductance in neuronal somata of *Helix*. *J. Physiol., Lond.* **254**, 129–151.

ECKERT, R. AND LUX, H. D. (1977). Calcium-dependent depression of a late outward current in snail neurons. *Science* **197**, 472–475.

ECKERT, R., TILLOTSON, D. L. AND BREHM, P. (1981). Calcium-mediated control of Ca and K currents. *Fedn Proc. Fedn Am. Socs. exp. Biol.* **40**, 2226–2232.

FINDLAY, I. (1988). Calcium-dependent inactivation of the ATP-sensitive K channel. *Biochim. biophys. Acta* **943**, 297–304.

GALVAN, M. AND SEDLMEIER, C. (1984). Outward currents in voltage-clamped rat sympathetic neurones. *J. Physiol., Lond.* **356**, 115–133.

GOLA, M., DUCREUX, C. AND CHAGNEUX, H. (1990). $Ca^{++}$-activated $K^+$ current involvement in neuronal function revealed by *in situ* single channel analysis in *Helix* neurones. *J. Physiol., Lond.* **420**, 73–109.

GOLA, M., DUCREUX, C. AND CREST, M. (1989). Involvement of calcium-activated K channels in the firing characteristics of molluscan neurons. *Pflügers Arch. ges. Physiol.* **414** (Suppl. 1), S142–S143.

GOLA, M., HUSSY, N., CREST, M. AND DUCREUX, C. (1986). Time course of Ca and Ca-dependent K currents during molluscan nerve cell action potentials. *Neurosci. Lett.* **70**, 354–359.

GOLA, M. AND ROMEY, G. (1971). Réponses anomales à des courants sous-liminaires de certaines membranes somatiques (neurones géants d'*Helix pomatia*). *Pflügers Arch. ges. Physiol.* **327**, 105–131.

GORMAN, A. L. F., HERMANN, A. AND THOMAS, M. V. (1982). Ionic requirements for membrane oscillations and their dependence on the calcium concentration in a molluscan pace-maker neurone. *J. Physiol., Lond.* **327**, 185–217.

GUSTAFSSON, B., GALVAN, M., GRAFE, P. AND WIGSTRÖM, H. (1982). A transient outward current in a mammalian central neurone blocked by 4-aminopyridine. *Nature* **299**, 252–254.

HERMANN, A. AND GORMAN, A. L. F. (1981). Effects of tetraethylammonium on potassium currents in a molluscan neuron. *J. gen. Physiol.* **78**, 87–110.

HEYER, C. B. AND LUX, H. D. (1976). Control of the delayed outward potassium currents in bursting pace-maker neurones of the snail *Helix pomatia*. *J. Physiol., Lond.* **262**, 349–382.

HOFMEIER, G. AND LUX, H. D. (1981). The time courses of intracellular free calcium and related electrical effects after injection of $CaCl_2$ into neurons of the snail, *Helix pomatia*. *Pflügers Arch. ges. Physiol.* **391**, 242–251.

IWATSUKI, N. AND PETERSEN, O. H. (1985). Inhibition of $Ca^{2+}$-activated $K^+$ channels in pig pancreatic acinar cells by $Ba^{2+}$, $Ca^{2+}$, quinine and quinidine. *Biochim. biophys. Acta* **819**, 249–257.

JIA, M., EHRENSTEIN, G. AND IWASA, K. (1988). Unusual calcium-activated potassium channels of bovine parothyroid cells. *Proc. natn. Acad. Sci. U.S.A.* **85**, 7236–7239.

KOSTYUK, P. G., DOROSHENKO, P. A. AND TSYDRENKO, A. Y. (1980). Calcium-dependent potassium conductance studied on internally dialysed nerve cells. *Neuroscience* **5**, 2187–2192.

KOSTYUK, P. G., KRISHTAL, O. A. AND DOROSHENKO, P. A. (1975). Outward currents in isolated snail neurones. I. Inactivation kinetics. *Comp. Biochem. Physiol.* **516**, 259–263.

KRAMER, R. H. AND LEVITAN, J. B. (1988). Calcium-dependent inactivation of a potassium current in the *Aplysia* neuron R15. *J. Neurosci.* **8**, 1796–1803.

LEVITAN, E. S. AND LEVITAN, I. B. (1986). Apparent loss of calcium-activated potassium current in internally perfused snail neurons is due to accumulation of free intracellular calcium. *J. Membr. Biol.* **90**, 59–65.

LUX, H. D. AND HOFMEIER, G. (1982*a*). Properties of a calcium- and voltage-activated potassium current in *Helix pomatia* neurons. *Pflügers Arch. ges. Physiol.* **394**, 61–69.

LUX, H. D. AND HOFMEIER, G. (1982*b*). Activation characteristics of the calcium-dependent outward potassium current in *Helix*. *Pflügers Arch. ges. Physiol.* **394**, 70–77.

MAGURA, I. S., KRISHTAL, O. A. AND VALEYEV, A. G. (1971). Behaviour of delayed current under long-duration voltage clamp in snail neurones. *Comp. Biochem. Physiol.* **40A**, 715–722.

MEECH, R. W. (1978). Calcium-dependent potassium activation in nervous tissue. *A. Rev. Biophys. Bioeng.* **7**, 1–18.

MEECH, R. W. AND STANDEN, N. B. (1975). Potassium activation in *Helix aspersa* neurones under voltage clamp; a component mediated by calcium influx. *J. Physiol., Lond.* **249**, 211–239.

ONOZUKA, M., IMAI, S., DEEURA, S., TAKEUCHI, H., FURUICHI, H., NISHIYAMA, K. AND OZONO,

S. (1988). Properties of a calcium-activated potassium channel in neurones of the snail *Euhadra peliomphala*. *Comp. Biochem. Physiol.* **91**A, 353–361.

PIN, T., CREST, M., EHILE, E., JACQUET, G. AND GOLA, M. (1990). Plateau-generating nerve cells in *Helix*: morphological and electrophysiological characteristics. *J. exp. Biol.* **152**, 189–209.

REUTER, H. AND STEVENS, C. F. (1980). Channel conductance and ion selectivity of potassium channel in snails neurones. *J. Membr. Biol.* **57**, 103–118.

RUBEN, P. AND THOMPSON, S. H. (1984). Rapid recovery from K current inactivation on membrane hyperpolarization in molluscan neurons. *J. gen. Physiol.* **84**, 861–875.

RUDY, B. (1988). Diversity and ubiquity of K channels. *Neuroscience* **25**, 729–749.

SCHWARZ, J. R. AND PASSOW, H. (1983). Ca-activated K channels in erythrocytes and excitable cells. *A. Rev. Physiol.* **45**, 359–374.

THOMAS, M. V. AND GORMAN, A. L. F. (1977). Internal calcium changes in a bursting pacemaker neuron measured with Arsenazo III. *Science* **196**, 531–533.

THOMPSON, S. H. (1977). Three pharmacologically distinct potassium channels in molluscan neurones. *J. Physiol., Lond.* **265**, 465–488.

THOMPSON, S. H. (1980). Inactivation of delayed K current. In *Molluscan Nerve Cells: From Biophysics to Behavior* (ed. J. Loester and J. H. Byrne), pp. 115–123. Cold Spring Harbor Laboratory Reports in the Neuroscience **1**.

TOKIMASA, T. (1985). Intracellular Ca-ions inactivate K-current in bullfrog sympathetic neurons. *Brain Res.* **337**, 386–391.

TSUDA, Y., OYAMA, Y., CARPENTER, D. O. AND AKAIKE, N. (1988). Effects of $Ca^{++}$ on the transient outward current of single isolated *Helix* central neurones. *Br. J. Pharmac.* **95**, 526–530.

VERGARA, C. AND LATORRE, R. (1983). Kinetics of Ca-activated K channels from rabbit muscle incorporated into planar bilayers. *J. gen. Physiol.* **82**, 543–568.

WOOLUM, J. C. AND GORMAN, A. L. F. (1981). Time dependence of the calcium-activated potassium current. *Biophys. J.* **36**, 297–302.

## Note added in proof

Our data indicate that delayed outward $K^+$ currents have a magnitude and inactivating properties that are characteristic of a cell type. Similar results were described by Serrano and Getting (1989) for the transient A current. From a quantitative study performed in various dorid neurones, they showed that the steady-state activating and inactivating processes of the A current were invariant between cells, while A current magnitude and inactivation kinetics varied in a cell-specific manner.

## Reference

SERRANO, E. E. AND GETTING, P. A. (1989). Diversity of the transient outward potassium current in somata of identified molluscan neurons. *J. Neurosci.* **9**, 4021–4032.